ELEVATION MODELING FROM SATELLITE DATA♦

Thierry Toutin
Canada Centre for Remote Sensing
588 Booth Street, Ottawa, Canada K1A 0Y7
Email: thierry.toutin@ccrs.nrcan.gc.ca

ABSTRACT

Most geoscientific applications using georeferenced cartographic data need a good knowledge and visualization of the topography of the Earth's surface. For example, mapping of geomorphological features is hardly feasible from a single image; three-dimensional (3D) information has to be generated or to be added for a better interpretation of the two-dimensional (2D) data.

Since the early emergence of earth observation satellites, researchers have investigated different methods of extracting 3D information using satellite data. Apart from a few early stereo-images acquired with hand-held cameras during the Gemini and Apollo missions, the first experiments to extract 3D data using stereo viewing from space began with the Earth Terrain Camera (ETC) flown onboard SkyLab in 1973-74.

Since these early experiments, various analog or digital sensors in the visible or in the microwave spectrum have been flown to provide researchers and geoscientists with spatial data for extracting and interpreting 3D information of the earth's surface. Although the shape-from-shading technique can be applied to optical sensor (OPS) images, stereo-viewing using space camera or digital scanner images was, and still is the most common method used by the mapping, photogrammetry and remote sensing communities.

However, side-looking synthetic aperture radar (SAR) data gives also the opportunity to extract 3D information using image-processing techniques appropriate to the nature of the data. With SAR data, three main methods have been developed: radargrammetry, clinometry and interferometry. Radargrammetry (similar to the stereoviewing of optical data) uses two images acquired from different viewpoints to generate a stereopair and stereoviewing. Clinometry takes advantage of the SAR shading and shadowing in the image, and interferometry uses mainly the SAR signal data instead of the image.

The paper will review the different methods and sensors used to extract absolute or relative elevation and assess their performance using the results from various research and commercial organizations. It will also discuss the respective advantages, difficulties and constraints of the sensors, the methods, and the technologies used to take into account the strength of each. It will also assess how they perform as complementary sources and systems for extracting elevation data in an operational context.

1. INTRODUCTION

At one time, a hilltop provided the best vantage point from which to observe nature's workings, but now discoveries in optics, photography and flight allow us to see the Earth as never before. Advanced methods in computing and signal processing technologies have enabled us to increase our ability to visualize, perceive and extract information from the Earth's surface. Today earth observation satellites orbit our planet collecting data to produce images, which allow us to monitor, understand and plan the use of our world's resources.

Remote sensing has evolved into an important supplement to ground observations and aerial photographs in the study of terrain features, such as the ground elevation. With the advent of instruments that produce images from electro-magnetic radiation beyond which the human eye and cameras are responsive, human "vision and perception" has been greatly extended (Lyon, 1966; Manual of Remote Sensing, 1998).

Why is it important that the third dimension be conveyed? Because humans are naturally able to see in three dimensions. The "naturalness" of a 3-D representation of reality enhances our ability to interpret 2D imagery. Cartographers, engineers, geologists, hydrologists, and other geo-scientists use different 3D viewing methods to perceive the ground elevation in order to better understand the Earth's surface. For example, representation of the third dimension supplies important information about the relationship between land shape and structure, slopes and waterways, surface material and vegetative growth.

A digital elevation model (DEM), which is a digital representation of the Earth's relief, is now one of the most important data structures used for geospatial analysis. Unfortunately, DEMs of usable details are still not available for much of the Earth, and when they are available they frequently lack sufficient accuracy. The digital format of a DEM made it easier to derive additional information for various applications, so that elevation modelling has become an important part of the international research and development (R&D) programs related to geo-spatial data.

Due to high spatial resolution of recent satellite sensors (Landsat–TM, SPOT-HRV, IRS-LISS, ERS-SAR, RADARSAT-SAR, etc.) a large number of researchers around the world have investigated the elevation modelling and the production of DEMs. There is plenty of literature describing the methods, algorithms and accuracy assessment of DEMs. Some examples are: Manual of Photogrammetry, 1980; Leberl, 1990; Williams, 1995; Polidori, 1996; Manual of Remote Sensing, 1998 or review articles (Day and Muller, 1988; Lemmens, 1988; Buchroithner, 1989; Maître *et al.*, 1997; Polidori et Toutin, 1998). They have addressed different, but generally not all, aspects of DEM generation from satellite data. A completely comprehensive and update review is not available at that time.

Furthermore, recent research into modelling computer vision on human vision has led to the advent of new alternative applied to satellite imagery. Current research in computer vision assumes that if a computer program can be made "to see" things as a human would, the algorithm must have some basis in human vision. Consequently, to better develop an understanding of the different methods used to derive elevation from satellite images the relationship between depth vision and perception and terrain elevation representation has first to be addressed. Only the basic concepts and the historical background of natural depth perception relevant for remote sensing applications are presented. The different methods (clinometry, stereoscopy, interferometry, polarimetry and altimetry) are then presented and their applicability to the variety of data reviewed (space photographs, digital sensor in the visible and infra-red (VIR) spectrum and SAR). Finally some concluding remarks on these methods and the future prospects of the next generation of satellites are presented.

2. HISTORICAL BACKGROUND AND BASIC CONCEPTS

2.1 Constructing the Third Dimension

Throughout history, humans have tried to represent what they saw and understood through images. Everything from cave walls, to canvasses, to computer screens have been used to express perception of our surroundings. Maps have provided one means of showing the relationship between humans and their environment. Towns, roads, rivers, mountains, valleys, and where the land meets the sea have been drawn in an organized fashion for centuries. Mapmakers have always sought ways in which to represent both the location and the 3D shape of land.

Mapmakers and other illustrators have traditionally used rendering techniques such as shading, overlapping and perspective views to create a 3D effect. Leonardo da Vinci (1452-1519) demonstrated in 1492 the principles of optical projection. His German contemporary, Albrecht Dürer (1471-1528), produced an outline of the laws of perspective, and in 1525 he constructed samples of mechanical devices with which he made true perspective drawings of nature scenes. His devices included an apparatus for producing stereoscopic drawing (Manual of Photogrammetry, 1980). In the last hundred years, many advances in representing three dimensions have been made. Stereo-models, anaglyphs or polarized images, chromostereoscopic images and holograms can provide 3-D information about our planet while 2-D flat images cannot.

2.2 Vision and Perception

For humans, the information provided by the eyes undoubtedly plays the dominant role in our interpretation of the environment. But the power to integrate the viewed image, to recognize its contour, its colour, and its relationship with other objects indicates that the process of vision does not merely consist of "seeing" but also of "perceiving" and understanding through the central nervous system. The eye, considered as part of the brain, is fundamentally an organizer. The eye/brain, starting with the activity of the retina, is actively building a world of objects: our mental model in psychology. This suggests that *a priori* knowledge is useful for a better interpretation and understanding of the image: to have a clear idea of what to look for, where to look, and how to look (Hoffman, 1990).

Perception, or perceiving, refers to the process whereby sensory stimulation is translated into organized experience. That experience, or precept, is the joint product of the stimulation and the process itself. In the "depth" context, the visual system (the process) creates the 3D world (the precept) we experience from the 2D pattern projected onto the retinas (the stimulation). But the fact that we can see depth quite well with one eye closed, or in a photograph or painting, indicates that two eyes are not necessary for a satisfying sense of depth. This dichotomy suggests an intimate relationship between what might be called "object recognition" and perception of three-dimensionality. Unfortunately, at this point, we know little about how the brain identifies objects, so a large portion of "depth perception" is not understood (Friedhoff and Benzon, 1991).

However, in modern psychology, it is accepted that depth perception is based upon four

physiological (accommodation, convergence, binocular disparity and motion parallax) and six psychological cues (image size, linear perspective, areal perspective, overlapping, shade and shadow, texture gradient) (Okoshi, 1976). These cues are treated as additional pieces of information which, when added to a flat picture on the back of the eye, make depth perception possible. The brain combines these cues in our mental model with the 2-D picture to produce judgements about the relationship of objects in space.

2.3 Depth Perception with Remote Sensing Data

Within the field of remote sensing if is generally recognized that psychological factors, such as perception, play a major role, but researchers devote little time or no time to studying the psychological aspects of the remote sensing processes (Hoffman, 1990). In fact, it has been shown that the interpretation of cartographic information can be facilitated by using 3-D or perspective representations when compared to a flat 2-D display (Bemis *et al.*, 1988). Since terrain relief modelling is based on the principal concepts related to the human depth perception, what are the main cues that play a role in depth perception of remotely sensed data?

Perspective is the most popular and widely used with remote sensing data. It combines different cues such as linear perspective, overlapping and texture gradient. It also takes advantage of the viewer's conceptual knowledge of the perspective phenomena. This psychological cue is thus only used for a representation and visualization of the terrain topography combined with remote sensing images and not for terrain modelling.

Shade and shadows are familiar phenomenon, which can help one to judge the size and shape of objects by providing profile representations. It is particularly helpful if the objects are very small or lack tonal contrast with their surroundings. For example, large look angle SAR images, which approximate low sun angle aerial photography in order to accentuate minute surface irregularities, are becoming important in geological investigations.

Shading is sometimes confused with shadowing. Shading is the variation of brightness exhibited in the image. It arises primarily because some parts of a surface are oriented so as to reflect more of the incident illumination towards the sensor (Horn and Brooks, 1989). Since shading provides cues all over the surface not just along special contours, this principle is used with the shape-form-shading technique to derive terrain slope and elevation. Shadow on a surface results when another surface intercepts the illumination from the source. It only provides localized cues (along special contours) to shape, although the shadow of a curved surface cast on another curved surface is very difficult to interpret. This principle is used to derive elevation of a specific target such as buildings, trees, etc.

Binocular disparity and convergence are the two physiological cues when viewing imagery in stereoscopy. Binocular disparity predominates with optical images because it reproduces the natural process of human binocular vision. It is important when viewing radar images, but the shade and shadow cues have also a strong and cumulative effect on stereo radar imagery. As an example on a quasi-flat terrain, the psychological cues overcome the binocular disparity when looking at the radar stereo-pair in pseudoscopy (apparent reversal of natural relief when inverting the viewing position of the two images) (Toutin and Amaral, 1999). Due to the specific

geometric and radiometric aspects of SAR images, it may take our brain time to assimilate this non-natural stereo viewing, mainly when both geometric and radiometric disparities are large (Toutin, 1998a). However, since depth perception is an active process (brain and eye) and relies on an intimate relationship with object recognition, with experience, radar images can be viewed in stereo as easily as VIR satellite images (Toutin and Vester, 1998). This principle is used in satellite photogrammetry and radargrammetry by computing the terrain elevation from the measured parallaxes (related to the binocular disparity) between the two images.

3. SHADOW AND SHADE FOR CLINOMETRY

3.1 Basic Concepts

Shadow has been used for a long time in astronomy. In 1610, Galileo observed Moon spots. The first ambiguity was to determine if these spots were shadows or low reflectivity surfaces. Looking at their evolution as a function of the sun illumination he concluded them as being shadows from the moon relief (Polidori, 1996). Later on, the height of craters was determined using the lengths of shadows of the crater edges (Rindfleisch, 1966).

One of the first applications of shape-from-shading was used in robot vision to detect the 3-D shape of industrial objects with diffuse reflecting surface. Using the principle that an image of a smooth object known to have a uniform surface will exhibit gradations of brightness, or shading, the shape can be determined to map the height of this surface. Because there are two degrees of freedom to surface orientation, the reflectivity does not uniquely determine the local normal but a set of possible normal directions. These directions describe a cone, whose axis is the illumination direction, and the half-angle the incidence angle. Consequently, local operation on the brightness alone cannot be used to determine the shape of the surface and its orientations. Additional constraint must therefore be added: generally the surface is assumed to be continuous and smooth, so that the surface orientations of neighbouring surface elements are not independent. If the reflectivity function and the position of the illumination source are known, the shape can thus be obtained from the shading.

The application of this concept to remote sensing data is less evident due to the sensitivity of shading to reflective properties of Earth's surface. Even if this reflectivity function has been described with data from many experimental observations (Teillet *et al.*, 1982; Ulaby and Dobson, 1988; Domik *et al.*, 1988), a general Lambertian model is often chosen for simplification when a small range of incidence occurs (Smith *et al.*, 1980). The local slope is then computed from the pixel reflectivity value and transformed into relative elevation by integration pixel by pixel. In other words, shape-from-shading makes uses of the sensitivity of micro-topography, but it cannot provide absolute location. Some reference elevation information is needed to derive the absolute elevation. More details for VIR or SAR sensors are given in the next Sections. In summary, the accuracy of this technique with remote sensing data is limited by intrinsic radiometric and geometric ambiguities:

1. The reflectivity is not only dependent on the local incidence angle, but also on the albedo related to land cover, rugosity, humidity, etc. as a function of the sensor. Miscalibration and SAR speckle are also a source of error.

2. The determined incidence angle yields to a set of potential orientations whose normal directions describe a cone. Furthermore this method only determines slopes, reference elevations have to be known, and the accuracy is limited by the height error propagation.

On the other hand, cast shadow and occluded areas can also be used to extract relative heights (La Prade and Leonardo, 1969; Cheng and Thiel, 1995) or to determine ground control points (Brivio *et al.*, 1992; Toutin *et al.*, 1998a). The shadow areas occur when the ground surface is not illuminated by the source ("backslope" related to the illumination source), and the occluded areas occur when the ground surface is not visible from the sensor ("backslope" related to the sensor). Since the illumination source is the sensor with SAR images the effects of these two concepts are mixed, but they are different with VIR images since the illumination source, the sun, and the sensor are different. While occluded areas are completely without information, shadow areas in VIR images have some information because the terrain receives some diffuse sun illumination partially reflected by the terrain. The impacts of shadow/occluded areas for VIR and SAR images are addressed in the next two Sections.

3.2 Application with VIR Images

For VIR images, shadow and occluded areas are different since the illumination source is the sun. Satellite VIR images are acquired from the descending path of a sun-synchronous orbit, and the local solar time is generally before or around noon (e.g., for SPOT, the local solar time of the descending node is around 10:30am). Consequently, west-looking images will have shadow and occluded areas in the same direction. Care must be taken to separate these two effects. Since the sun elevation angle around noon will generate shadow with steep slopes it can be consistently measured only from vertical structures such as buildings or trees (in a row or isolated), or very rough terrain. However with a low sun elevation angle (in wintertime) the relief perception of a rugged terrain is inverted (Saraf *et al.*, 1996). Occluded areas could be only used to extract elevation information with off-nadir viewing images, but this has been never addressed.

This method using shadow length measurements is largely used with aerial photos in which the pixel resolution is much better than the object height (Huertas and Nevatia, 1988). To our knowledge no attempt has been realized with space photographs. Knowing the sun and sensor geometry, the same method can be applied to VIR images, such as panchromatic SPOT images, even if the resolution is coarser (Cheng and Thiel, 1995). Using a simple trigonometric solution, they compute elevation with 3.7-m accuracy over a sample of 42 well-defined buildings. A correction for the known terrain slopes was also introduced. Since the shadow length is manually measured at the pixel unit (10 m for panchromatic SPOT image) these good results can be accounted for by the size of the building (up to 60 m with a mean of 30 m), and the large shadow cast (up to 18 pixels with a mean of 8 pixels). Hartl and Cheng (1995) computerized the method and applied it over a complete city. Only 30% of over 78800 buildings were extracted, with calculated heights less than 20 m for 90% of them. Seventy-seven buildings were randomly selected to check their height error. The root mean square error was about 6 m, with only 11 buildings having errors larger than 10 m (SPOT resolution). The high building density and the overlapping of grey value were the main factors leading to the larger error.

Since shadow boundary is a key point in the process, different tools have been developed to determine it more accurately. Meng and Davenport (1996) created an edge-image template using the point-spread function of the sensor. After a manual rough location of the edge, a correlation process between the template and the actual image determines the best location of the shadow edge within $1/100^{th}$ of a pixel. Unfortunately no ground truth data has been provided for checking the accuracy.

On the other hand, Shettigara and Sumerling (1998) developed a four-step process using the spatial information of a panchromatic SPOT image and the spectral information of the infrared band of a SPOT image. Firstly, an appropriate threshold to delimit shadows in the images is selected. Shadows cast by rows of trees are used to estimate the mean heights of trees. Calibration curves are then constructed to relate the actual mean heights of trees to the estimated heights. Finally, heights of industrial buildings are computed using their shadow lengths and the calibration curves, without any correction for the terrain slopes. A 3-m accuracy has been measured with only three 12-m tall buildings. Although the shadow determination is more sophisticated, the results are similar to the first method (Cheng and Thiel, 1995). The advantage of this method, when compared to the first one is that the shadow boundaries are located with sub-pixel accuracy using an optimum threshold that enables smaller building heights to be estimated. The disadvantages are that two SPOT images are used, and some ground data for the trees-row heights are necessary to determine the calibration curves. Conversely, the first method does not use ground data for height estimation. No attempt to verify the method over a complete city in a real environment has been attempted, as with the first method (Hartl and Cheng, 1995).

Shape-from-shading can be applied to VIR imagery since information concerning the terrain is contained in multi-scanner data. With homogeneous surfaces where variations in reflectance may only refer to topographic surface differences, rather than to land cover effect, a simple reflectance model can be used to derive the topographic information. Lodwick and Paine (1985) used two Landsat-1 and 2 images (July and October) over an ice cap on Baffin Island, Canada to obtain high and low sun angles and maximum difference in sun azimuth. They considered for the reflectivity with a simplified Lambertian model (Teillet *et al.*, 1982) and two empirical models to resolve the radiometric ambiguity. The slopes being in the sun-azimuth direction resolved the conic ambiguity. They first demonstrated with a training sample that the reflectance conditions of an ice cap are non-Lambertian for a large range of incidence angles, such as Smith *et al.* (1980) for pine forest cover types. The first empirical model used a second order polynomial computed over training samples. Difficulties in obtaining representative training samples were the main source of errors even if high correlation was obtained. The second empirical model applied a simple linear model between typical maximum slopes in the "sun facing and away facing" directions and the reflectance values at the one-percent level of the grey value histogram. It was the best solution to generate height differences, which broad agreement to values observed on the map.

Finally a weighted third-order surface adjustment is carried out with nine control points to transform the 50-m posting slopes in the sun-azimuth direction into elevations. The results for the basic shape of the ice cap surface compared well with the base map. Some variations could be partly explained by the surges (melting and re-freezing) of the ice-cap surface. No quantitative accuracy results have been given due to the lack of precise and digital topographic

information.

These qualitative results should have generated some interest in the scientific community to expand on this work. However, no other results with different study site and data sets have been presented to date. It seems that most of the research effort in the applicability of the method has been directed towards SAR data.

3.3 Applications with SAR Images

For SAR images, shadow and occluded areas are mixed, since the illumination source is the sensor itself. Therefore they are completely without information and the boundaries of a cast shadow are easier to determine than with VIR images. Depending on the SAR look angles, only the steepest slopes produce shadow/occluded areas. Height determinations can then be made for the same type of vertical structures (buildings, rows of trees, etc.) for which such measurements have been made on VIR imagery. La Prade and Leonardo (1969) used simple trigonometric models and knowledge of the SAR geometry to translate measured shadows into heights. However, layover lengths have to be added to the shadow lengths to take into account the good positioning of the base of the vertical structure.

Cast shadows provide only localized cues to shape. On the other hand shade provides cues all over the surface, not only along special contours. This radiometric information (the radar backscatter) of each image pixel is used in radar clinometry to determine the local orientation of the terrain and then the elevation by the integration of slopes.

Radar clinometry, as an adaptation of photoclinometry developed by Horn (1975), has been further developed by Wildey (1984) for the mathematical equations, then again by Wildey (1986) for its operational feasibility in anticipation of the Magellan mission to map Venus. Radar clinometry capabilities and limitations are well known, even if the research studies have been limited (Frankot and Chellapa, 1987, 1990; Thomas *et al.*, 1989; Guindon, 1990). At first, the principle appears simple: essentially the inversion of a mathematical expression of the radar backscatter in terms of the albedo and the local incidence angle. As mentioned previously, there are more severe limitations due to intrinsic radiometric and geometric ambiguities when the method is applied to SAR images of general terrain surfaces, and not only to homogeneous surfaces such as in the previous experiment with VIR images (Lodwick and Paine, 1985).

The first radiometric ambiguity is related to the inversion of the model since it depends on two parameters. The SAR backscatter of the surface is altered if the surface properties vary from place to place. In this case assuming uniform reflecting properties (constant albedo) will recover a shape (incidence angle) that is different from the actual one. This approximation, as an extension of the photo clinometry, was also used with SAR by Wildey (1986) and Frankot and Chellapa (1988). More sophisticated models (Domik *et al.*, 1988; Ulaby and Dobson, 1988; Boisvert *et al.*, 1995), which take into account the SAR and surface interaction (surface geometry, vegetation, soil properties, geographic conditions, etc.) have been developed. They should now permit one to establish a more realistic backscattering model of the intensity (Paquerault et Maître, 1997) than the traditional Lambertian model used for a homogeneous surface (Keidel, 1982). No attempt to use them has been made due to a relative decline of the

method in the scientific community during the last decade. Other radiometric problems that are not completely controlled and fully resolved are specific to SAR sensors (Polidori, 1991; Paquerault et Maître, 1997): namely speckle, miscalibration and "discretized" sampling.

The conic ambiguity is related to the definition of the incidence angle. Even when accurately determined, it does not uniquely define the orientation of the surface but a set of possible orientations. Their normal directions describe a cone with the axis being the illumination direction. Since there are two degrees of freedom to surface orientation, it takes two numbers to specify the direction of a unit vector perpendicular to the surface (Horn, 1975). One brightness measurement at each picture cell only gives one equation for two unknowns at every cell. Additional constraint or assumption has to be made to resolve this conic ambiguity. One assumption implemented by Widley (1986) is the hypothesis of local cylindricity. It enforces a local continuity between adjacent pixels to define a local cylinder. Since there is no iteration in the solution process, the local-cylindricity method is sensitive to integration approximations and image noise. It then tends to accumulate these effects along the full DEM reconstruction leading to "pseudo systematic" errors (Leberl, 1990).

Other assumptions or constraints to resolve the conic ambiguity implemented by Frankot and Chellapa (1988) are the notions of integrability and regularization. The first one states that heights can be integrated along any path since these values are independent of the integration path. This constraint acts as a smoothing process. The second one limits the amount of allowable oscillation in the computed terrain surface. Furthermore, they used an iterative approach starting from an approximate existing DEM. Differences between grey values of the real image and the SAR synthetic image, predicted from the latest estimated DEM, are used to improve the terrain's slopes and heights and to converge to the final DEM. In conjunction with the two previous integrability and regularization constraints, this approach tends to spread out the speckle noise errors instead of propagating them.

Thomas and Kober (1990) expanded this iterative approach to multiple images. Some spot heights derived from stereoscopy or other sources can also be added as supplementary constraints of the estimated heights. Using multiple image algorithms give better stability and robustness with noisy images during the iteration procedure, as well as a faster convergence. However, it does not fully resolve the two basic ambiguities.

For the conic ambiguity, Guindon (1990) quantitatively demonstrated that the SAR image grey level is not an effective indicator of local incidence angle, and hence is not an accurate measure of the overall local terrain surface normal direction. It is only a strong indicator of the range component of the terrain slope. It can therefore only be used to derive elevation profiles for individual image range lines. Since no significant detectable information is available about azimuthal slope, an additional source of "azimuthal control" data is required to tie the adjacent range line elevation profiles to a common and absolute origin. Paquerault et Maître (1997) thus developed a two-step strategy to compute these two components of the incidence angle. Firstly, they computed the range component from the backscatter grey level pixel, and integrated it along a range line. They then applied a contextual Markovian strategy to successively modify, in a random order, each pixel orientation of the full image. This second step enabled them: (i) to take into account the azimuth component of the incidence angle, (ii) to link together the adjacent

range lines elevation profiles, and (iii) to reduce the noise error propagation.

Despite the developments in the mid-1990's, SAR shape-from-shading remains a marginal technique, applied mainly in difficult situations such as tropical land cover or extra-terrestrial sites without ground truth. This is mainly due to the fact that the radiometric ambiguity between the terrain albedo, the radar backscattering cross-section and the incidence angle is rarely solved, except on an homogeneous terrain surface with a Lambertian model. However, a large part of the Earth, without cartography, approximates to these homogeneous surfaces.

4. BINOCULAR DISPARITY FOR STEREOSCOPY

4.1 Basic Concepts

In about the year 1600, the German astronomer Johannes Kepler (1571-1630) gave the first precise definition of stereoscopy, and a Florentine painter Jacopo Chimenti produced one of the first hand-drawn stereo-picture pairs (Wicar Museum, Lille, France, circa 1600).

In modern photogrammetry, "*stereoscopy is the science and art that deals with the use of images to produce a three-dimensional visual model with characteristics analogous to that of actual features viewed using true binocular vision*" (La Prade *et al.*, 1980).

In the stereoscopic space perception, two major cues are used: the convergence and the binocular disparity. Convergence is the ability to focus the optical axes of the two eyes on to a single object. The sensing of the amount of muscular tension in the eyes resulting from different convergence angles provides a cue to the absolute distance to the viewed point. The binocular disparity (or parallax) is the disparity or the "difference" between the images of an object projected on to each retina. The degree of disparity between the two projected images depends on the convergence angle. The binocular disparity is considered the most important perception cue over medium distance, and is the only one used in stereo photo- or radargrammetry for quantitative elevation extraction.

The three main applications of stereoscopy are:
1. The interpretation aid in qualitatively recognizing the 3D form of an object;
2. The quantitative estimate of slopes and relative heights; and
3. The quantitative and precise measurements of three-dimensional co-ordinates of planimetric and altimetric features.

In the last 50 years, first optico-mechanical, and later analytical and digital 3-D photogrammetric systems capitalizing on the binocular parallax and convergence cues have been developed for aerial photographs to meet the needs of these three applications of stereoscopy (especially the latter). It was U.V. Helava, who developed the main concepts behind these analytical and digital systems in 1957. Most of the stereo workstations have now been adapted to process stereo data from the same satellite sensors (space photo, VIR or SAR), but only few can simultaneously process mixed sensor stereo pairs. Stereo images displayed on the screen are separated either spatially, radiometrically or temporarily. Photogrammetric principles for space photos (co-linearity and co-planarity conditions) and their equivalent for remote sensing data

mathematically solve the relationship between 2-D image co-ordinates and 3-D ground co-ordinates. The hardware and software to derive information from the 2-D digital imagery has thus allowed the mapping process to become more automated (Helava, 1988a), but not completely, with occasional unmatched expectations (Grün, 1997).

Among all the new developments of the stereo workstations, DEM generation is an important R&D topic. In fact, any satellite data can be used to generate a stereoscopic pair and simulate the natural depth perception, as soon as the terrain is imaged from two different viewpoints. Since the stereoscopic methods to extract elevation, based on the binocular disparity and parallax, are "more or less" the same, stereoscopic capabilities of different sensors are first analyzed. The processing, the methods and the error propagation are then addressed.

4.2 VIR Sensors

Two main categories of VIR sensors have to be considered: the space cameras and the digital scanners.

4.2.1 Space Cameras

For a long time, space camera technology remained in the military domain. Since the techniques and technologies of space photographs are derived from classical aerial photographs, photogrammetrists have postulated that space cameras would be the next logical step for topographic mapping.

The first significant satellite photogrammetry experiment was done using imagery on the Apollo 15, 16 and 17 missions to the moon. A lunar control net with 30-m relative accuracy in the three co-ordinate axes was generated, and 1:25 000 topographic ortho-photo maps were produced (Doyle, 1979). After a few early stereo hand-held photographs acquired during the Gemini and Apollo missions, the Earth's Terrain Camera (ETC) experiment onboard Skylab-D in 1974 produced the first along-track stereo-viewing images from space. One of the first attempts to measure heights from space images was made by Mott (1975). He reported a root mean square error (RMSE) of 120 m for a strip of four Skylab models and concluded that the minimum contour intervals to be plotted should be approximately 250 m.

The ETC was followed by the German Democratic Republic's MKF-6M multi-band camera flown on the Soviet spacecraft, Soyuz 22 and Salyut in 1976. None of these were metric cameras (MCs) capable of producing acceptable accuracy, even with an image pixel size of 17 m to 30 m. Furthermore, wide gap spaces between ground tracks hinder the mappinf of large areas (Kostka, 1986; Buchroithner, 1989).

In 1978, the USSR flew the KATE140 MC on Salyut acquiring panchromatic images with 60-m resolution. Later the USSR developed RESURS a series of remote spacecraft based on the recoverable Vostok capsule. They carried different multi-band MC (KATE-200, KFA-1000, LK-1000 and MK4) with retrievable film on missions lasting between two and four weeks. The ground resolution varies from less than 5 m to 30 m. At the same time, the German Zeiss MC initiated by the European Space Agency (ESA) took panchromatic and near-infrared images

during the Space Shuttle STS-9 mission between November 28 and December 7, 1983. Later on, the ITEK Large Format Camera (LFC) initiated by the National Aeronautics and Space Administration (NASA) was flown on the Space Shuttle STS-41-G on October 5-10, 1989. The LFC has a Forward Motion Compensation (FMC) system to produce a better image quality.

Since these different metric cameras have along-track stereo-capabilities, elevation can be derived. However, most of the research work has been on the estimation of the stereo acuity (Doyle, 1979, Kostka, 1986, Buchroithner, 1989), or on the evaluation of planimetric and altimetric accuracies over a limited number of points (Meneguette, 1985). Other results were reported by various authors at the Metric Camera Workshop held in Oberpfaffenhofen, Germany in February 1985, or at the ACSM-ASPRS Annual meeting held in Washington, D.C., USA in March 1986. They mainly used an analytical stereo-plotter for which Earth curvature correction has been added to the normal photogrammetric bundle adjustment, but not for varying atmospheric conditions (Jacobsen and Müller, 1988).

Two experiments generated contour lines, one with MC data (Ducher, 1985) and the other with LFC data (Murai, 1986), both on analytical stereo-plotters. In the first experiment, 50-m contour lines have been digitally plotted and compared with 1: 25 000 topographic maps. It shows a standard error of about 30 m with larger errors in the steepest areas. In the second experiment, difficulty in extracting 20-m contour lines was reported. The height accuracy of the extracted contour lines was only computed from 30 points, and was 15 m in average for stereo-pairs with a base-to-height (B/H) ratio of more than 0.6. Although less significant, these LFC stereo-pair results are better due to the FMC system. The obtained accuracy was in the same order as the predicted accuracy for generating contour lines at 20-m to 30-m intervals with LFC data (Doyle, 1979), but it does not completely meet the requirements of cartography, particularly in mountainous areas (Kostka, 1986).

The main reasons why these data have not been used for operational DEM production are (Ducher, 1985):

- the limited distribution of the data relative to the amount of acquired images;
- the experimental nature of the data and system, and the lack of decision to make it fully operational and repetitive; and
- the relatively poor quality of the data.

Consequently the stereo capabilities of the MC and LFC camera have mainly become a source of planimetric feature content for mapping using traditional photogrammetric techniques with analytical stereo-plotter (Whittington, 1989).

4.2.2 Digital Scanners

To obtain stereoscopy with images from satellite scanners, two solutions are possible:

1. the along-track stereoscopy from the same orbit using fore and aft images; and
2. the across-track stereoscopy from two different orbits.

The last solution was the most used since 1980: first, with Landsat from two adjacent orbits, then with SPOT using across-track steering capabilities, and finally with IRS-1C/D by “rolling” the

satellite. In the last few years, the first solution as applied to space frame cameras, gained renewed popularity. Examples are, the JERS-1 OPS, the German Modular Opto-Electronic Multi-Spectral Stereo Scanner (MOMS), the Advanced Spaceborne Thermal Emission and Reflection Radiometer (ASTER), the IRS-P5, and most of the high-resolution satellites such as Orb-View1 and Quick-Bird. Only Ikonos will have simultaneously along- and across-track capability.

4.2.2.1 "Adjacent Orbit" Stereo

In the case of Landsat (MSS or TM), the stereoscopic acquisition is only possible from two adjacent orbits since the satellite acquires nadir viewing images, and the tracking orbit ensures repeat path consistent within a few kilometres. In fact, since the mean B/H ratio with Landsat-MSS is around 0.1, one needs relief of about 4 000 m to generate a parallax of five Landsat-MSS pixels (80-m resolution). Due to its quasi-polar orbit, the coverage overlap grows from about 10% with a B/H ratio of 1.8 at the Equator to about 85% with a B/H ratio of 0.03 at 80º latitude. From 50º north and south the coverage overlap (45%) with a B/H ratio less than 0.12 enables quasi-operational experiments for elevation extraction. Welch and Lo (1977) extracted elevation of ten control points from different colour-photograph stereo-pairs acquired from Landsat-1. They designed a precise parallax-bar instrument with various viewing magnifications (10x to 30x), and obtained a RMSE for the elevation between 300-500 m. They noticed a large error in the parallax difference measurements on the analog photographs. Digital processing should thus allow a better parallax measurement accuracy.

Simard (1983) and Simard and Slaney (1986) then used digital Landsat-MSS and Landsat-TM stereo-pairs, respectively with a B/H ratio of 0.11 over the mountains (2,000-m elevation variation) in British Columbia, Canada. Ehlers and Welch (1987) also applied the method using Landsat-TM data with a larger B/H ratio (0.17) over a low relief (500-m elevation variation). For the three experiments, the images are first corrected for the geometric distortions related to the platform, sensor and look geometry. The residual misregistration (or parallax) between the images of the stereo pair thus reflects the relief effect. Cooper *et al.* (1987) also suggested correcting for the Earth curvature, if it is not done. Since the east-west component accounts for almost 98% of the total parallax, a simplified one-dimensional model to compute the elevation from the measured parallax can be used (Simard, 1983):

$$dh(x, y) = dp(x, y)\ H/B \qquad (1)$$

Where dh and dp are the relative height and parallax at each image point (x, y), respectively.

This equation can be modified for the different orientation of the scan lines, but the variation in B/H is less than 0.004 (Ehlers and Welch, 1987). These models are an approximation of the stereo geometry, which is only good because of the coarse satellite image resolution (30-80 m), the poor B/H (0.1-0.2) and the final expected accuracy (50-100 m).

The parallax for each pixel is measured using a hierarchical cross-correlation technique with variable reference window size (Simard, 1983). The window size for the search window can also be adjusted according to image content and signal-to-noise ratio (Ehlers and Welch, 1987).

More details on the method are given in section 4.5.

Qualitative and visual evaluation of the resulting DEM or the derived contour lines show generally good agreement when overlaid on the ortho-rectified Landsat-MSS imagery (Simard, 1983) or with the existing map contour lines (Ehlers and Welch, 1987). Quantitative evaluation gives a RMSE of about 45 m when compared with independent check points (ICPs) (Simard and Slaney, 1986; Ehlers and Welch, 1987), and of 60 m to 70 m with a low precision 1:250 000 map derived DEM (Cooper *et al.*, 1987). The resulting variations of this last study can be accounted for by the low precision map DEM, and from the correlation process using edge matching instead of grey level matching. More details on the correlation results and performances are given in section 4.5.

The stereoscopic capabilities with Landsat data still remain limited because:

- it can be applied for large areas only in latitude higher than 45º to 50º north and south;
- it generates a small B/H ratio leading to elevation errors of more than 50 m; and
- only medium to high relief areas are suitable for generating sufficient vertical parallax.

4.2.2.2"Across-Track" Stereo

To obtain good geometry for better stereo plotting, the intersection angle should be large in order to increase the stereo exaggeration factor, or equivalently the observed parallax, which is used to determine the terrain elevation. According to Light *et al.* (1980), B/H ratios of 0.6 to 1.2 are a typical value to meet the requirements of topographic mapping. The SPOT system with its across-track steering capabilities (±26º) can generate such B/H ratios. In conjunction with a finer pixel size (10 m for panchromatic image) a more precise model has to be used to transform the parallax extracted from the raw SPOT images into an elevation value. Since the perspective of the SPOT push-broom scanner is a conico-cylindrical perspective (conical for imaging a line and cylindrical for the displacement of the satellite), new geometric and stereoscopic models, equivalent to co-linearity and co-planarity equations in photogrammetry, have to be developed for the generation of a precise DEM. To transform image co-ordinates or parallax into map co-ordinates, the parametric model has to take into account:

- the distortions relative to the platform (position, velocity, orientation);
- the distortions relative to the sensors (orientation angles, instantaneous field of view, detector signal integration time);
- the distortions relative to the Earth (geoid-ellipsoid including relief); and
- the deformations relative to the cartographic projection (ellipsoid - cartographic plane).

Some of the first studies were undertaken at the Institut Géographique National, France from raw-type simulated stereo SPOT data generated by the Centre National d'Études Spatiales (CNES), the French Space Agency (Guichard, 1983; Masson d'Autumne, 1984; Toutin, 1985). These three studies reported 3-m accuracy both in planimetry and altimetry with the simulated stereo-pair (B/H ratio of about 1.1). Furthermore, 20-m contour lines were generated using automatic correlation, and qualitatively compared to contour lines generated from aerial photographs with an analytical stereo-plotter (Masson d'Autumne, 1984). Quantitative results have also been presented using the Matra Traster analytical stereo-plotter with the same

simulated SPOT stereo-pair (Vigneron et Denis, 1984), and showed an elevation error of 5 m with 80 % confidence.

Simulation works of georeferenced-type SPOT data were also done in Canada (Simard, 1981). He generated a DEM with a RMSE of 5.7 m from geo-referenced stereo images corrected for systematic distortions (satellite, sensor, Earth curvature and rotation) with a B/H ratio of 0.5. Other studies with simulated SPOT images were later conducted around the world (US, UK, Australia, Sweden etc.) using analytical stereo-plotter or automatic correlation methods (Vincent *et al.*, 1984; Cooper *et al.*, 1987).

After the launch of SPOT-1 in February 1986, CNES sponsored the SPOT Preliminary Evaluation Program (PEPS) to assess SPOT capabilities for thematic and topographic mapping. In preparation for the launch and early PEPS data, considerable research was carried out to develop robust and rigorous mathematical models describing the specific acquisition geometry of the SPOT-HRV sensors (Masson d'Autume, 1979; Khizhnichenko, 1982; Guichard 1983; Toutin, 1983; Konecny *et al.*, 1986; Gugan, 1987; Kratky, 1987; Paderes *et al.*, 1989 and Westin, 1990) and others.

Most of these researchers used the photogrammetric solution (co-linearity conditions for the conic perspective of a single image line), and took into account the displacement of the satellite (cylindrical perspective) to link the equations. Since the parameters of neighbouring lines are highly correlated, and satellite positions and attitude can be computed from on-board recording systems, the mathematical equations can be reduced to a minimum of eight to ten unknowns depending on the development and implementation of the solution. Only some of them have been adapted to process stereo-data (co-planarity condition).

Most of the results with real data were presented at the SPOT-1 Image Utilization, Assessment, Results Symposium held in Paris, France in November 1987 (CNES, 1987). Academic research results rather than operational systems or projects dominated the Conference. In general, an accuracy of 10 m or less for the planimetry and the elevation was achieved. The differences are mainly dependent on the accuracy of the SPOT geometric modelling and its implementation in the workstation since good cartographic data were generally used. For DEM generation two main processing methods have been presented:

- using an analytical stereo-plotter; or
- using a digital image analysis system.

The first method uses a stereo analysis system with SPOT data on transparency photographs. Following the Traster System developed by Matra in conjunction with IGN, France for the software aspects (Vigneron and Denis, 1984), different universities or mapping agencies around the world developed solutions in collaboration with photogrammetric instrument manufacturers: the Kern DRS-1 (Gugan and Dowman, 1988), the Zeis Planicomp (Priebbenow and Clerici, 1987; Konecny *et al.*, 1987), the Wild Aviolyt (Trinder *et al.*, 1988), and the Canadian NRC Anaplot-1 (Kratky, 1989). Contour lines can be interactively stereo-plotted to further generate DEM. Petrie (1990, 1992) are good references on the progress of analytical stereo workstations and their processing capabilities. Later, Hottier and Albattah (1991) described a method by re-

sampling raw SPOT stereo images to generate a pair of quasi-epipolar images that is suitable for stereo plotting on an analog stereo-plotter. The processed stereo-image pair was thus plotted on a Wild AG1 without either excessive Y-parallax or significant loss of information.

When digital photogrammetric workstations became more available the different analytical solutions and software were ported into these fully digital systems. Some of them also took advantages of low-cost personal computers (Welch, 1989; Toutin *et al.*, 1993; Toutin and Beaudoin, 1995). Dowman *et al.* (1992), Heipke (1995) and Walker and Petrie (1996) are good references on the progress of digital stereo workstations and their processing capabilities.

The second method uses fully digital images and processing without any stereo-viewing capabilities most of the time. The DEM is automatically derived from the digital SPOT images using correlation techniques and a geometric SPOT model, (Gugan and Dowman, 1986; Denis, 1986; Guichard *et al.*, 1987; Renouard, 1987; Simard *et al.*, 1987) and others.

The Indian Remote Sensing satellites (IRS) 1C and 1D also have across-track stereo capability. This is achieved by rolling the satellite rather than steering the instrument. In anticipation of the planned stereo IRS-1C data, Malleswara *et al.* (1996) used the "adjacent orbit" stereo technique with the IRS-1A linear imaging self-scanning sensor data, which does not have across-track stereo capability. Using the same methodology with Landsat data (geo-referenced data, least square matching and approximated elevation modelling) they generated a DEM over three study sites with stereo images displaying various overlaps (16% to 27%) and B/H ratio (0.12 to 0.14). The DEMs was then checked with 30 ICPs, and showed an error with 90% confidence of about 35 m with a slight correlation between the error and the B/H. Jacobsen (1997) carried on the investigation with three IRS-1C images (two off-nadir, B/H = 0.8 and one nadir) over Hannover, Germany. When compared to over 80 ICPs he obtained an accuracy of ±1.1 pixels (6.5m) in planimetry and elevation. No DEM was extracted. The results are worse than those generally obtained with SPOT or with other IRS-1C data because:

- they used a non-parametric solution instead of using a rigorous photogrammetric solution adapted to the specific geometry and characteristics of the LISS sensors (Toutin *et al.*, 1998b; Cheng and Toutin, 1998); and
- the attitude data are not always consistent and accurate (Toutin *et al.*, 1998b).

Few results on DEM extraction have been published, due to the limited availability of stereo IRS images. Cheng *et al.*, (1999) generated a DEM (least square matching, rigorous photogrammetric modelling) from raw IRS-1C LISS stereo-images (B/H = 0.52) over a mountainous area in Arizona, USA (elevation variation of 2 100 m). They reported an elevation accuracy of about 10 m when compared both to ICPs and digital DEM of the United States Geological Survey (USGS). It is still worse (1.7 corresponding pixels) than results on the same type of relief with SPOT (about one corresponding pixel or better). This is most likely due to the inconsistent attitude data. Further work with IRS-1D could provide a better answer if stereo-data were more available to researchers.

4.2.2.3 "Along-Track" Stereo

Launched in 1992, JERS had the capability to acquire along-track stereo-images by the use of forward and nadir linear array sensors, named OPS. The 15º forward-looking image and the nadir-looking image (18-m ground resolution) generate a stereo-pair with a B/H ratio of 0.3. The simultaneous along-track stereo-data acquisition gives a strong advantage in terms of radiometric variations versus the multi-date across-track stereo-data acquisition. It was confirmed by the very high correlation success rate (82.6%) (Raggam and Almer, 1996), which can compensate for the weaker stereo geometry.

Few results on DEM extraction from JERS data (Raggam and Almer, 1996; Westin, 1996) have been presented after the first Japanese experiment (Maruyama *et al.*, 1994). All experiments have generated DEMs with the correlation method and photogrammetric solutions. Although the methods used are approximately the same, Westin (1996) obtained results (20 m) twice as good as Maruyama *et al.*, (1994) or Raggam and Almer (1996). This 20-m accuracy corresponds to one pixel spacing, which needed an automatic parallax measurement accuracy of better than one-third of a pixel with the 0.3 B/H ratio. Even when the GCPs were separated from over 200-km distance on the same image strip, the interpolated distance and the distribution of the control data did not affect the elevation accuracy.

The German MOMS is another push-broom scanner with along-track stereo capability. This development started with MOMS-1 in 1979, with the first experiment flown mainly as a technical verification of the instrument line. In a second step, experimental MOMS-2 data (ground resolution of 13.5 m) were acquired during the German space lab mission in 1993 for testing the map generation potential. Since the system has fore-and-aft scanners (±21º) a B/H ratio of 0.8 can be obtained. Both methods, with an analytical plotter (Dorrer *et al.*, 1995) and with a digital correlation (Ackerman *et al.*, 1995) have been used over an Australian test site to produce 10-m and 5-m intermediate contour lines and DEMs, respectively. Checked only with ICPs a DEM error of 16 m was measured. Qualitative evaluation of the contour lines achieved very good consistency (even for the 5-m contour lines) with the ground truth. It thus enables scales up to 1:25 000 to be mapped. These better results are accounted for by the superiority of human depth perception when compared to automatic correlation techniques with this data set (Dorrer *et al.*, 1995). Due to the bad quality of the control data in the Australian data set, they both expected to consistently improve the height accuracy to 5 m with the third MOMS-2P/PRIRODA mission to be flown on the Russian space station MIR. However, the first experiment with this third mission data (18-m resolution and 0.8 B/H ratio) showed a degradation on the DEM accuracy to 25-30 m (Raggam *et al.*, 1997) while a second experiment achieved a 10-m accuracy (Kornus *et al.*, 1998). The large discrepancy between these two last experiments can be accounted for by the different type of relief or/and by the different geometric modelling of the 3D-array scanner. Future studies will confirm the potential accuracy of this VIR scanner.

4.2.3 SAR Sensors

In the 1960's, stereoscopic methods were first applied to radar images to derive ground elevation leading to the development of radargrammetry (La Prade, 1963). He showed that some specific SAR stereo configurations would produce the same elevation parallaxes as those produced by air photos. Consequently, elevation could be derived on traditional stereo-plotters. They can only

be used to measure target elevations. Furthermore, Carlson (1973) developed a single path technique to generate radar stereo images, which made it easier to view and to measure parallax for elevation computation than the traditional two-path technique. However, the lack of radar stereo-pairs led mainly to theoretical studies (Rosenfield, 1968; Gracie *et al.*, 1970; La Prade, 1970; Leberl, 1979) or simulated data processing experiments (Kaupp *et al.*, 1983; Domik, 1984).

During the 1980's, improvements in SAR systems, with parallel investigations into the theory, have allowed the demonstration of stereo radar with same-side or opposite-side viewing. These theoretical studies and practical experiments (Leberl, 1976) confirm that the opposite-side stereo configuration is superior to same-side stereo configuration. The difficulty in using these geometrically superior configurations stems from the illumination differences that are too pronounced to be stereoscopically viewed and the difficulty of finding corresponding points and features. Figure 1 illustrates the intersection geometry with the radar parallax due to elevation for different stereo configurations (same versus opposite side; steep versus shallow look angles).

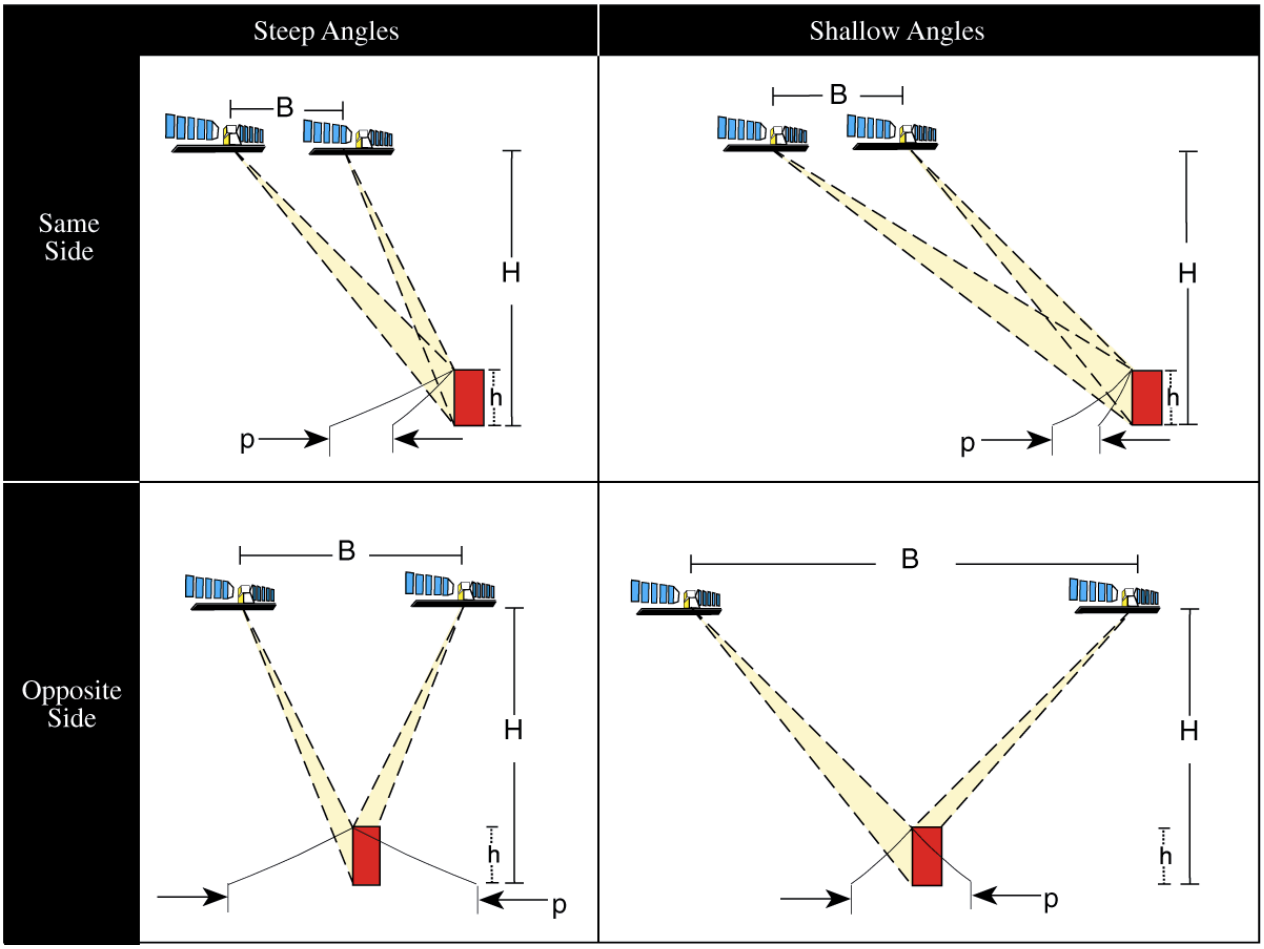

Figure 1: The intersection geometry with the radar parallax (p) due to the terrain elevation (h) for different stereo SAR configurations (same side versus opposite side; step versus shallow look angles).

To obtain good geometry for better stereo plotting, the intersection angle (Figure 1) should be large in order to increase the stereo exaggeration factor, or equivalently the observed parallax, which is used to determine the terrain elevation. Conversely, to have good stereo viewing, the interpreter (or the image matching) prefers a stereo-pair as nearly identical as possible, implying a small intersection angle. Consequently, large geometric and radiometric disparities both hinder stereo-viewing and precise stereo plotting. Since the reduction of one disparity could compensate for the other disparity, a compromise has to be reached between better stereo viewing (small radiometric differences) and a stronger geometry and plotting (large parallax).

The common compromise for any type of relief is to use a same-side stereo-pair thus reducing both disparities. Unfortunately, this does not optimize the full potential of stereo radar for all terrain topography. A compromise to reduce the radiometric difference of an opposite-side stereo-pair is to invert the radiometry of one image (Yoritomo 1972; Fullerton *et al.*, 1986). When processing digital images, Fullerton *et al.*, (1986) added a local brightness change to exclude some image features from the radiometric inversion. A low frequency or a sparse DEM can also be used to reduce the geometric disparity, as it has been applied with success to iterative hierarchical SAR image matching (Simard *et al.*, 1986). Another potential compromise is to use opposite-side stereo-pair over rolling topography (Toutin, 1996). The rolling topography reduces the parallax difference and also the radiometric disparities (no layover, shadow and little foreshortening) making possible the stereo viewing and a good stereo plotting.

However, with spaceborne platforms, parallel flights (from opposite or same side) are very rare. Even sun-synchronous satellite orbits are only parallel near the Equator. Elsewhere, crossing flight lines or convergent stereo configuration must be considered. No differences exist between computations for parallel flight lines and those for crossing flight lines, if rigorous intersection geometry is applied. That has been confirmed with the SIR-A and -B shuttle missions of 1981 and 1984 (Kobrick *et al.*, 1986; Leberl *et al.*, 1986a; Simard *et al.*, 1986). The two first studies processed radar photographs on an analytical stereo-plotter, the Kern DSR-1, which was adapted to process stereo SAR images (Raggam and Leberl, 1984). The third study used a fully digital method with iterative hierarchical matching. The results achieved for the DEM were in the order of 60 m to 100 m due mainly to the poor SIR-A resolution, or radiometric and geometric image quality. Furthermore with the SIR-B SAR system stereo-pairs with intersection angles ranging 5º to 23º can be created (Leberl *et al.*, 1986b).

Since the launch in the beginning of the 1990's of different satellite sensors (Almaz, ERS, JERS, etc.) radargrammetry again became a hot R&D topic. First, the Russian Almaz-1 SAR system could have acquired images with different angles to obtain stereo-images in the latitude range from 0º to 72º. Yelizavetin (1993) digitally processed two images with 38º and 59º look angles acquired over a mountainous area of Nevada, USA. No quantitative results were given. Stereoscopy with ERS-SAR data is obtained using an image with its normal look angle (23º) and a second image with the Roll-Tilt mode angle (35º) to generate a same-side stereo-pair (Raggam *et al.*, 1993; Twu and Dowman, 1996). It can also be done with two normal look angle (23º) images from ascending and descending orbits to generate an opposite-side stereo-pair (Toutin, 1995; 1996). Comparison of these research results, 20 m versus 40 m (Marinelli *et al.*, 1997) confirmed the superiority of the opposite-side stereo-pair. With the JERS-SAR, stereoscopy has

been obtained with adjacent orbits generating a small overlap with a small intersection angle (Raggam and Almer, 1996). The digital correlation method was used to generate a 75-m accurate DEM.

Results obtained with simulated and spaceborne SAR data can be summarized as follows:

1. Kaup *et al.* (1983) found that the optimum intersection angles are about 40º - 45º;

2. Domik (1984) showed that the best subjective stereo impressions were obtained with shallow look angles (50º - 70º), and at an intersection angle of 20º;

3. Leberl *et al.* (1986a, b) showed that the highest accuracy is not necessarily achieved with the largest intersection angles;

4. Fullerton *et al.*, (1986) noted that higher ground resolution does not necessarily lead to higher height accuracy; and

5. Better accuracy is more consistently achieved with opposite side stereo-pair (Fullerton *et al.*, 1986; Toutin, 1996; Marinelli *et al.*, 1997).

These reported results are inconsistent and practical experiments do not clearly support theoretical expectations: for example, larger intersection angles and higher spatial resolution do not translate into higher accuracy. In various experiments, accuracy trends even reverse, especially for rough topography. Only in the extreme case of low relief, does accuracy approach theoretical expectations.

By analogy with photogrammetry, theoretical error analyses were first developed by Rosenfield (1968) and La Prade (1970). They related an error of an exterior orientation element in the left and right images to the resulting error in the stereo model. These first analyses were mainly limited to absolute errors, and to comparing same-side with opposite-side stereo. Leberl (1979) had a more general approach for the error propagation, identifying both relative and absolute errors regardless of the stereo configuration. As a summary, an estimation of the error in the cross-track and elevation co-ordinates, E_x and E_h respectively, due to an error in range, E_r, for the measurement of a target in the stereo model is given by:

$$E_x = [(\cos^2 \theta_L + \cos^2 \theta_R)^{1/2} / \sin \Delta\theta] E_r \qquad (2)$$

$$E_h = [(\sin^2 \theta_L + \sin^2 \theta_R)^{1/2} / \sin \Delta\theta] E_r \qquad (3)$$

Where θ_L and θ_R are the look angles of the left and right images respectively, and $\Delta\theta$ is the intersection angle as being the difference between the two look angles.

As shown in Equations 2 and 3, the error modelling accounts only for SAR geometric aspects (look and intersection angles, range error) and completely neglects the radiometric aspects (SAR backscatter) of the stereo-pair and of the relief. This error propagation modelling can then only be applied when the radiometry has a minor role and impact with respect to the geometry, such

as during the stereo model set-up with GCPs, which are radiometrically well defined points (Sylvander *et al.*, 1997; Toutin, 1998b). The residuals error of the least square adjustment of the stereo model are thus correlated with the intersection angle.

Since SAR backscatter, and consequently the image radiometry, is much more sensitive to the incidence angle than the VIR reflectance, especially at low incidence angles (Polidori and Toutin, 1998), the theoretical error propagation has a major limitation as a tool for predicting accuracy and selecting appropriate stereo images for DEM generation. Care must therefore be taken in attempting to extrapolate VIR stereo concepts to SAR.

Before RADARSAT, Canada's first earth observation satellite was launched in November 1995, it was difficult to acquire different stereo configurations to precisely address this point, namely the impact of radiometry in the error propagation. RADARSAT (Figure 2) with its various operating modes, imagery from a broad range of look directions, beam positions and modes at different resolutions (Parashar *et al.*, 1993) fills this gap. Under the Applications Development and Research Opportunity (ADRO) program sponsored by the Canadian Space Agency (CSA), researchers around the world have undertaken studies on the stereoscopic capabilities by varying the geometric parameters (look and intersection angles, resolution, etc.). Most of the results were presented at the final RADARSAT ADRO Symposium held in Montreal, Canada in 1998 (CSA, 1998). There was general consensus in the results of the DEM extraction accuracy: a little more than one resolution for the fine mode (12 m), and little better for the standard mode (20 m), whatever the method used (digital stereo-plotter or image correlation). Relative elevation extraction was also addressed from a fine mode RADARSAT stereo pair for the measurements of canopy heights in the tropical forest of Brazil (Toutin and Amaral, 2000).

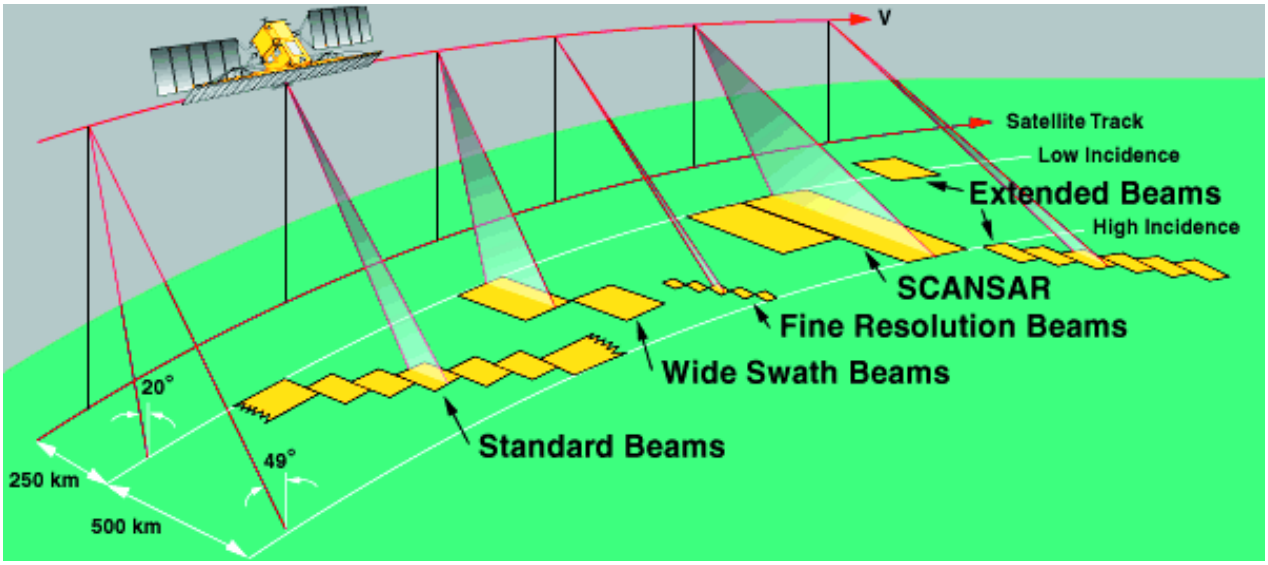

Figure 2: Operating modes of RADARSAT-SAR.

However, there was no significant correlation between the DEM accuracy and the intersection angle or the vertical parallax ratio (Toutin, 1999). In fact, most of the results showed that the principal parameter that has a significant impact on the precision of the DEM is the type of the relief (and its slopes) (Toutin, 2000a). The greater the variation between two look angles (e.g. 23° and 47°), the more the quality of the stereoscopic fusion deteriorated. This cancels out the advantage obtained from the stronger stereo geometry. On the other hand, although a higher resolution (fine mode) produced a better quality image, it does not change the stereo acuity for a given stereo configuration (e.g. intersection angle), and it does not significantly improve the DEM accuracy. Furthermore, although the speckle creates some confusion in the stereo plotting, it does not degrade the DEM accuracy because the correlation method or the human stereo viewing "behaves like a filter". Pre-processing the images with an adaptive speckle filtering does not improve the DEM accuracy (Dowman *et al.*, 1997); it can slightly reduce the image contrast and smoothes the relief (especially the low relief) (Toutin, 1999).

Since the type of relief is an important parameter in the DEM accuracy, it is strongly recommended that the DEM accuracy be ascribed values that reflect the different areas of the relief. Furthermore, in the choice of a stereoscopic pair for DEM generation, both the geometric and radiometric characteristics must be jointly evaluated taking into account the SAR and surface interaction (surface geometry, vegetation, soil properties, geographic conditions, etc.). The advantages of one can compensate for the deficits of the other.

4.2.4 Mixed Sensors

Due to the increasing amount of image data, it is very common to have data from different sensors over the same terrain area. The traditional stereoscopic technique can be thus applied. By perceiving the different radiometry in the brain the stereoscopic fusion of mixed sensors can also provide a virtual 3D model of the terrain surface. Few results have been published on the use of mixed stereo sensors to generate DEMs. Welch *et al.*, (1990) used a 23° viewing angle SPOT image (band 3) and a Landsat-TM image (band 4) with the automatic stereo correlation capability of the Desktop Mapping System (Welch, 1989). Comparison of profiles for the stereo extracted DEM with the existing 1:50 000 topographic maps indicated a RMS error of about ± 100 m. This large error is mainly due to the polynomial co-registration process instead of a rigorous parametric geometric model. In fact, Raggam and Almer (1991) generated a 50-m accurate DEM from a 23º viewing angle SPOT image (band 1) and a Landsat-TM image (band 2). A proper relative registration process was used to generate the epipolar images for the measurement of corresponding image points with an automatic stereo correlation process. They reported 65% success rate in the correlation step due to the radiometric difference between the two images and to homogeneous nature of some areas (snow fields, glacier or shadow). Human interaction is still required to reject blunders or to fill the mismatched areas in order to optimize the DEM results. This requires a digital stereo workstation, not only with automatic matching, but also with full stereoscopic capabilities (GCP and tie points stereo-plotting, 3-D DEM editing, 3-D cartographic feature extraction, etc.) (Toutin, 1998c).

In fact, the brain can generate the perception of depth combining, for example, the spatial information from a SPOT panchromatic image and the spectral information from a Landsat-TM

image for stereo plotting when image matching fails. Toutin (1998c) reported an altimetric accuracy of 37 m for the elevation data extracted from a raw 26°-viewing angle SPOT-P and Landsat-TM (band 1) stereo-pair. The 10-m resolution of the SPOT-P image, and the fact that elevation data are extracted directly from the raw image (no polynomial co-registration or epipolar image resampling) account for the better results. More difficulties have been reported by Akeno (1996) when trying to generate a DEM from a NOAA-AVHRR and Landsat-MSS stereo pair due to the large resolution difference (1 km versus 80 m). He registered the two images using image-to-image correlation and degraded the Landsat-MSS image to the AVHRR resolution. He reported 320-m accuracy over the good matched DEM points. The main difficulty was to obtain the sub-pixel accuracy in the correlation process, applied in the NOAA-AVHRR image rectification and the parallax measurement.

When two optical images are not available, a stereo-pair can be generated and viewed by combining optical and SAR images. Moore (1969) first addressed the principle theoretically. He used simultaneously acquired infrared line-scanner and SLAR images. In neither case was the visual stereo effect perfect except near 45° viewing angle. Various scaling factors were also applied to different areas of the stereo-pair to obtain the proper stereo effect for the height determination. No quantitative measurement was achieved due to the lack of an "adapted" stereo-plotter.

Further evaluation was done with SIR-B and Landsat-TM images (Bloom *et al.*, 1988). Only moderate results over 27 extracted points were reported, mainly due to pixel offset error in the registration of the images and the approximated angular values used in the simplified elevation computation equation. Using a better parametric solution, Raggam *et al.*, (1994) extracted a DEM from a multi-band SPOT and airborne SAR stereo-pair. Since no meaningful results can be obtained from automatic image correlation, they interactively measured 500 corresponding image points and computed the elevation off-line. Results of the comparison with a reference DEM showed a standard deviation of 60 m with a 42-m bias and minimum/maximum errors of about ±250 m. More recently, Toutin (1999b) further investigated the mapping feasibility of mixed sensor stereo-pairs with parametric geometric solutions ported into a fully digital stereo workstation adapted to process on-line VIR and SAR stereo-pairs. From the raw images (no epipolar resampling), the data are interactively stereo extracted, and then directly compared to a checked DEM. An accuracy of 20 m with no bias and minimum/maximum errors of less than ±100 m has been achieved from two different SPOT-P and ERS-SAR stereo-pairs: one being an opposite-side stereo-pair and the other a same-side stereo-pair. The full on-line stereo capabilities in the GCPs plotting and elevation measurements account for the good results. Comparisons of the two stereo-pair results showed that the elevation parallax, which contributes to the determination of the elevation, is mainly dominated by the SAR geometry with its high sensitivity to the terrain relief. Conversely, the radiometry of the SPOT-P images mainly contributes to the determination of the features with the quality of the image content.

4.3 Processing, Methods and Errors

The different processing steps to produce DEMs using stereo images can be described in broad terms as follows:

1. to acquire the stereo image data with supplementary information such as ephemeris and attitude data if available;

2. to collect GCPs to compute or refine the stereo-model geometry;

3. to extract the elevation parallax;

4. to compute the 3-D cartographic co-ordinates using 3-D stereo-intersection; and

5. to create and post-process the DEM (smoothing, filtering, 3-D editing, etc.).

Steps 2 and 4 involve mainly geometric issues, and step 3 involves radiometric issues while steps 1 and 5 involve both geometric and radiometric issues. Since the stereo-model geometry computed from the GCPs and step 4 are related and dependent of the type of images they are addressed in step 1.

4.3.1 Acquiring Stereo-Image Data

With VIR images two types of data can be used: raw images with only normalization and calibration of the detectors (e.g. level 1A for SPOT), or geo-referenced images (e.g. level 1B for SPOT) corrected for the systematic distortions due to the sensor, the platform and the Earth rotation and curvature.

Raw 1A imagery is preferred by photogrammetrists for use in analytical or digital stereo-workstations. As mentioned previously, the geometric modelling solution employs the well-known co-linearity and co-planarity equations. They have been adapted to suit the geometry of scanner imagery, but also have benefited from theoretical work in celestial mechanics to better determine the satellite's osculatory orbit and parameters (Escobal, 1965; CNES, 1980). More details on the development of the solutions and their implementation in the workstations can be found in the different referenced papers.

Since they have been systematically georeferenced the "level 1B" images just retain the elevation parallax. To compute the cartographic 3-D co-ordinates (Step 4) the 3-D stereo-intersection modelling is then reduced with a simpler 2-D polynomial-based solution for the planimetry, and separately with a simple parallax equation solution for the elevation (Eq. 1). This method was mainly applied in the first experiments with Landsat (Simard, 1983; Cooper *et al.*, 1987; Ehlers and Welch, 1987) since the approximation generated by the method is smaller than the final expected accuracy. However with SPOT stereo-images (better resolution and larger B/H ratio) the approximation is no longer valid and generates poorer results than with "raw" stereo images (Gugan and Dowman, 1988; Al-Roussan and Petrie, 1998). The solution to overcome this approximation when using 1B stereo-images is to convert the 1B-images back into 1A-images using the reverse transformation (Al-Roussan *et al.*, 1997), or to "re-shape and re-size" the 1B-images to the raw imagery format (Valadan Zoej and Petrie, 1998). This 1B-geometric modelling can be mathematically combined with the normal 1A geometric modelling to avoid multiple image re-sampling. Although this mathematical procedure used for 1B stereo images works better than the simple parallax approximation, it is still recommended that raw

stereo-images with the rigorous parametric solution (co-linearity and co-planarity equations) be used.

The SAR images are standard products in slant or ground range presentations. They are generated digitally during post-processing from the raw signal SAR data (Doppler frequency, time delay). The ground range presentation is the most popular product since the pixel spacing on the ground is roughly the same for the different look angle images. It then facilitates the stereo viewing and matching. The geometric modelling solution to compute the stereo-model and 3D intersection starts generally either from the traditional Doppler and range equations (Twu and Dowman, 1996; Sylvander *et al*., 1997), from the equations of radargrammetry (Leberl, 1990), or from generalized equations (Toutin, 1995). Their mathematical developments are different, and also depend on the method used (e.g. analytical or digital stereoworkstation, digital image or visual matching).

4.3.2 Collecting GCPs

Whatever the VIR and/or SAR geometric modelling used for the stereo model and 3D intersection, some GCPs have to be acquired to refine the stereo-model with a least square adjustment process in order to obtain a cartographic standard accuracy. Since the polynomial modelling does not reflect the geometry of viewing it requires many GCPs (20 and more) spread over the full stereo-pair. Each image modelling is computed separately, which does not set-up a relative orientation between the images. Furthermore the elevation is computed from an approximated solution. Consequently this modelling cannot be used to provide the high cartographic accuracy required with the last generation of satellite such as SPOT, IRS, MOMS, ERS, and RADARSAT.

With a parametric modelling such as those defined previously, few GCPs (1 to 6) are required. In an operational environment their number will vary as a function of their accuracy. They should preferably be spread at the border of the stereo pair to avoid extrapolation in planimetry. It is also preferable to cover the full elevation range of the terrain. Different types of GCPs can be used:

- full control points with known XYZ co-ordinates;
- altimetric points with known Z co-ordinate; and
- tie points with unknown cartographic co-ordinates.

The two last types are useful to reinforce the stereo geometry and fill in gaps where there is no XYZ GCP. Furthermore, GCPs displayed only on one image in or outside the stereo pair can also be acquired as complementary points to the “stereo” GCPs. Combined with tie points they can also help to avoid extrapolation in planimetry in areas where there is no “stereo” GCP.

The final accuracy of the stereo geometry is mainly dependent on the GCP’s cartographic and image co-ordinates. The first can be obtained from global positioning system (GPS), air photo surveys, map digitizing, etc. The image co-ordinates are plotted interactively on the plotter or the screen. Since some workstations do not have full stereoscopic capabilities, the image co-ordinates are obtained simultaneously in “double monoscopy”. This plotting will then create artificial X- and Y-parallaxes (few pixels) between the images, and the parallax errors will

propagate through the stereo model (relative and absolute orientations), the stereo-intersection and finally the DEM. The error propagation is much larger with a SAR stereo-pair than with a VIR stereo-pair where the plotting accuracy is about 1/3 pixel and the B/H ratio around one. Due to the same-side geometry with small intersection angles (8º to 20º) of SAR stereo-pairs this error propagation due to the "double monoscopic" plotting increases with shallower look angles and smaller intersection angles (Toutin, 1998b). Consequently the DEM accuracy can decrease with a 20% to 40% ratio, depending on the stereo-pair geometry (Toutin, 1999). True stereoscopic plotting using human depth perception enables a better relative correspondence of the GCP between the images (SAR but also VIR) and a better absolute positioning on the ground. It is also a requisite that the two images are computed together, and not separately, to obtain a relative orientation between them.

4.3.3 Extracting Elevation Parallax

Two main methods can be used to extract the elevation parallax using image matching: the computer assisted (visual) or automatic methods. These two methods can be of course be integrated to take into account the strength of each one.

The computer assisted visual matching is an extension of the traditional photogrammetric method to extract elevation data (contour lines) on a stereo-plotter. It requires full stereoscopic capabilities to generate the on-line three-dimensional reconstruction of the stereo model and the capture in real time of 3-D planimetric and elevation features. For elevation, the contour lines or an irregular grid DEM can be generated. The stereoscopic viewing is completed on the computer screen using a system of optics. The stereo images are separated spatially, radiometrically or temporarily. Spatial separation is achieved using two monitors or a split screen and an optical system using mirror and/or convex lenses. Radiometric separation is achieved by anaglyphic or polarization techniques with coloured or polarized lenses, respectively. Temporal separation is achieved by an alternate display of the two images and special synchronized lenses. Petrie (1992), Dowman *et al.* (1992), Audet et Lapierre (1993), Heipke (1995) and Walker and Petrie (1996) present the latest developments in analytical and digital stereo workstations these last twenty years. Furthermore, Makarovic (1990) gives a comprehensive comparison between analytical and digital techniques and systems.

To retain real 3-D performance in a stereo-workstation, the images are re-sampled into an epipolar or quasi-epipolar geometry, in which only the X-parallax related to the elevation is retained (Masson d'Autumne, 1979; Baker and Binford, 1981). Another solution to control the image positioning from the raw imagery is to automatically follow the dynamic change by cancelling the Y-parallax using the previously computed stereo-model (Toutin *et al.*, 1993; Toutin, 1995). In the same way as with a conventional stereo-plotter, the operator cancels the X-parallax by fusing the two floating marks (one per image) on the ground. The system then measures the bi-dimensional parallax between the images for each point, and computes the XYZ cartographic co-ordinates using the 3D intersection. The visual matching then combines in the brain a geometric aspect (fusing the floating marks together) and a radiometric aspect (fusing the floating marks on the corresponding image point). Some automatic tasks (displacement of the images or cursors, prediction of the corresponding image point position, etc.) are added.

However, computer-assisted visual matching, principally used with paper-format images and analytical stereo-workstations, is a long and expensive process to derive DEM. When using digital images automated image matching can thus be used. Since image matching has been a lively research topic for the last twenty years, an enormous body of research work and literature exists on stereo matching of different VIR and SAR sensors.

Most of the research studies on satellite image matching are based on David Marr's research at the Massachusetts Institute of Technology (MIT), USA into the modelling of human vision (Marr, 1982). If a computer program can be realized to see things as a human would, then the algorithm must have some basis in human visual processing. The stereo disparity is based on "correct" assumptions about the real world (Marr and Poggio, 1977): (i) a point of the surface has a unique position in space at any one time, and (ii) matter is cohesive. The first generation of image matching based on these assumptions is the grey-level image matching. Grey level matching between the two images really implies that the radiometric intensity data from one image, representing a particular element of the real world, must be matched to intensity data from the second image, representing the same real-world element.

Although satellite image of the real world represented by grey levels is not like a random-dot stereogram (easily matchable), grey level matching has been widely studied and applied to remote sensing data. Most of the matching systems operate on reference and search windows. For each position in the search window, a match value is computed from grey level values in the reference window. The local maximum of all the match values computed in the search window is the good spatial position of the searched point. The match value can be computed with the normalized cross-correlation coefficient (Simard, 1983), the sum of mean normalized absolute difference (Ramapriyan *et al.*, 1986), the stochastic sign change or the outer minimal number estimator, etc. The first one is considered to be the most accurate (Leberl *et al.*, 1994) and is largely used with remote sensing images. They also noticed that matching errors were smaller with SPOT images and digitized aerial photographs than with SAR images. The last two match value computation methods have been rarely or never used by the remote sensing community.

Another solution to the problem of matching, introduced by Förstner (1982), is the least-squares approach minimizing the squares of the image-grey level differences in an iterative process. This method makes possible the use of well-known mathematical tools and the estimation of the error. Rosenholm (1986) found that the more complicated least squares method applied on simulated SPOT images did not give any significant improvement when compared to the cross-correlation coefficient. However, this least-square method seems to be more accurate with real SPOT data (Day and Muller, 1988). No attempts have been made with SAR images.

The notion of least squares matching in the object domain (ground) rather than in the image domain was later introduced by Helava (1988b). Predicted image densities, corresponding to each ground element "groundel", are mathematically computed with known geometric and radiometric image parameters, and matched to the original one. The uncertainty in the parameters of a particular groundel is resolved by least squares. An advantage of this approach is to use more than two images from the same or different sensors to make the least squares solution meaningful, and a disadvantage is the ability to correctly model the groundel attributes for each image. It is mainly used with air photos since more than two images overlap the same

ground area and their geometry and radiometry are better controlled.

Since one of the constraints was either missing or incorrectly implemented in grey level matching, Marr developed a second generation of image matching: feature-based matching (Marr and Hildreth, 1980). The same element of the real world may look considerably different in remote sensing images acquired at different times and with different geometry between the sensor, the illumination and the terrain. Instead, edges in the images reflect the true structures (Cooper *et al.*, 1987). Feature-based matching has not been very popular in the remote sensing community, but successful applications have been achieved with simulated SPOT and Landsat-TM (Cooper *et al.*, 1987). The DEM results were not as good as those obtained by Simard and Slaney (1986) with Landsat-TM stereo-pair using grey level matching. Hähn and Förstner (1988) also found that least-square matching is more accurate than the feature-based matching, conversely to Marr's theoretical prediction.

Hybrid approaces can be thus be used to achieve better and faster results by combining the grey-level matching, the feature-based matching with a hierarchical multi-scale algorithm, and also with the computer-assisted visual matching. The feature-based approach may produce good results for identified features, but no elevation at intermediate points. They can then be used as seed points for the grey-level matching. Another hybrid approach is to generate gradient amplitude images as a first step with grey-level values derived from the original stereo-images instead of gradient images with only binary edge values. In a second step, any grey-level matching technique can be used on these pre-processed images (Paillou and Gelautz, 1998). The linear gradient operator can be designed to be optimal to remove noise (such as the SAR speckle) and to enhance edges. Their first preliminary results with SAR stereo-images show 10-15% improvement in the DEM reconstruction, not always significant or consistent, but at least with less blunders due to the noise removal.

Although the computer-assisted visual matching is a long process, it has been proven to be more accurate with photos or VIR data (Raggam *et al.*, 1994; Dorrer *et al.*, 1995) and with SAR data (Leberl *et al.*, 1994; Toutin, 1999, 2000b). It thus can be used either to eliminate the blunders, to fill the mis-matched areas or in areas where the automated image matching gives errors larger than one pixel (about 10% for SPOT, 15% for digitized photographs, and 40-50% for SAR images, Leberl *et al.*, 1994). It can also be used to correct the lake elevations or to generate seed points for the automatic matching.

Other developments tested principally for airborne images, but rarely with satellite images, include the global approach, scale space algorithms, relational matching, consideration of breaklines, multiple image primitives, etc. Some other research studies used the recognition of corresponding structures (Della Ventura *et al.*, 1990) or of uniform regions (Petit-Frère, 1992; Abbassi-Dezfouli and Freeman, 1996), a moment-based approach with a fine-invariant features (Flusser and Suk, 1994), or a wavelet transform approach (Djamdji and Bijaoui, 1995). They were only used to extract well-defined GCPs for image registration between different spaceborne VIR images.

More development could be done to integrate these solutions for generating seed points to grey-level matching. Some apparent contradictions should also be the issue of future research studies,

such as:

- the theoretical prediction of Dave Marr (1982) that the feature-based matching is better than the grey-level matching versus better experimental results with the grey-level matching than with the feature-based matching;
- the theoretical automated image matching error (much better than one pixel) versus the experimental results (one and more depending on the data); and
- the "so-called" superiority of computer matching over the visual matching versus the experimental results, etc.

These overall comments confirm our first statement that the image matching has been a lively research topic for the past twenty years and it may be for the next twenty years!

5. Other Methods

5.1 Interferometry

Radar interferometry is an alternative to the conventional stereoscopic method for extracting relative or absolute elevation information. It uses the advantages of SAR systems and of digital image processing: all-weather, night and day capabilities, and automated or semi-automated processing. Imaging radar interferometry combines complex images recorded either by two antennas at different locations or with the same antenna at two different times. The phase difference information between the SAR images is used to measure changes in the range, on the sub-wavelength scale, for corresponding points in an image pair. By analyzing the phase variations these distances can be translated into elevation or displacement on the ground. Since the interferometric techniques are largely detailed in another Chapter of this Encyclopædia of Analytical Chemistry: Instrumentation and Applications (Massonnet, 2000), only the basic aspects are given for understanding and comparing them with previously developed methods.

The first proposal and experiments in radar interferometry were in the field of planetary mapping in the context of radar astronomy (Rodgers and Ingalls, 1969). They used an Earth-based range-Doppler system to map Venus, and the interferometric information was only used to resolve the ambiguity in the mapping of southern and northern hemispheres. The first airborne application was done by Graham (1974) with two antennas carried on an aircraft. "Classified" until 1980, the technique was later extended to SIR-B data acquired from two separate passes acquired over several days (Gabriel and Goldstein, 1988). After the launch of ERS-1 in 1991, numerous multi-pass satellite interferometric studies have been accomplished (Massonnet and Rabaute, 1993; Zebker *et al.*, 1994a), afterwards with Almaz-1 (Yelizavetin and Ksenofontov, 1996) and with RADARSAT (Geudtner *et al.*, 1997). With existing satellite SAR data, only the repeat-pass system (one satellite antenna and two passes) can consistently generate interferometric data through the combination of complex images since there is presently no satellite system with two antennas. Dual-antenna system data are only available from the 10-day Shuttle Radar Topography Mission (SRTM) realized in February 2000.

The images are registered and the phase difference is computed for each pixel. The main product is the interferogram (phase difference), and the secondary product is a coherence image,

which indicates the correlation between the two SAR images. The phase difference, which is related to the two-way path difference of the radar echoes, is only known with a 2π ambiguity. It is then necessary to "unwrap" the phase differences for the determination of the absolute interferometric phase to within a constant (Goldstein *et al.*, 1988). The terrain elevations can thus be derived using an accurate SAR imaging model. However, there are geometric and radiometric limitations in the computation of the terrain elevation since the phase difference contains several components: topographic, atmospheric, displacement and noise.

To resolve these ambiguities and to address these different components, different developments in SAR interferometric processing took place, first with airborne SAR data in the 1980's and later with spaceborne. These include:

- the impact of the interferometric baseline on the elevation accuracy (Li and Goldstein, 1990);
- the evaluation of different atmospheric phenomena and the way to characterize them (Massonnet and Feigl, 1995);
- the differential interferometry combining multiple interferograms to estimate sub-centimeter surface displacement (Gabriel *et al.*, 1989);
- the time interval between the image acquisition (Vachon *et al.*, 1995).

Current developments also include the use of satellite radar interferometry to study dynamic phenomena and their relative elevation displacement. Combining a SAR interferogram generated from two ERS-1 SAR data acquired before and after an earthquake with a DEM, the topographic component is removed from the interferogram, and the displacement field of an earthquake is mapped (Massonnet *et al.*, 1993). Topographic and displacement components can also be separated by combining three radar images to generate two interferograms (Zebker *et al.*, 1994b). The estimation of the displacement field using radar data alone, without any terrain information is then possible. Similarly using repeat-track interferometry with very small cross-track baseline, which generates an interferogram with little sensitivity to topography (small topographic component), Goldstein *et al.* (1993) measured and estimated ice sheet motion. This technique is currently applied to RADARSAT data from the Antarctica mapping mission to measure ice motions (Gray *et al.*, 1998) and to analyze glacier flow dynamics (Forster *et al.*, 1998).

So far, the atmospheric component and the image coherence are the main limitations of the interferometric method for operational DEM generation. The coherence image can been also used as SAR interferometric signatures for land use classification with ERS-1 SAR repeat-pass data (Wegmüller and Werner, 1995). The interferometric correlation over forested areas was found to be significantly lower than over open canopies, small vegetation, bare soils and urban areas. The results strongly support deforestation studies, forest mapping and monitoring since it was possible not only to distinguish coniferous, deciduous and mixed forest stands, but also regrowth and clear-cut areas.

Although these results indicated that the scene coherence over forested areas was low, the interferometric technique has been used to estimate the topography and tree heights in specific conditions: a boreal forest in wintertime where the coherence varies from 0.2 to 0.5 (Hagberg *et al.*, 1995). The interferometric phase information used to estimate the tree height relative to an

open field and compared with *in-situ* measurements demonstrated that the scattering centre at C-band is close to the top of the trees if the forest is dense. The good coherence obtained is also a result of the stiffness of the "frozen" branches on the top of the boreal forest during the wintertime. They also noticed increased sensitivity of the degree of coherence to other environmental parameters (temperature, precipitation, snowfall and soil moisture change).

5.2 Polarimetry

SAR polarimetry has been used with success for thematic classification studies involving natural scenes and manufactured targets. A recently developed application of the SAR polarimetry involves both a direct measure of terrain azimuthal slopes and a derived estimate of the terrain elevations (Schuler *et al.*, 1996). The method is mainly based on empirical comparisons, supported by preliminary theoretical analysis, between the terrain local slope and the co-polarized signature maximum shift. This has been validated over different geographical areas and different types of natural targets using different DEMs as reference. Although it was only tested with airborne P- and L-band SAR platforms, it is worthwhile to mention it, since future satellite missions (ENVISAT, RADARSAT-2) will generate dual-polarimetric or full polarimetric SAR data.

Polarimetric SAR measures the amplitude and phase terms of the complex scattering matrix. Based on a theoretical scattering model (Valenzuela, 1968) for tilted, slightly-rough dielectric surfaces, azimuthal surface slope angles and signature-peak orientation displacements produced by such slopes are proportional over a range of azimuthal slopes. Empirical studies showed that an azimuthal angle of a open-field terrain caused a proportional shift of the co-polarized polarimetric signature maximum from its flat position by an angle almost equal to the terrain slope (Schuler *et al.*, 1996).

Since forest scattering is more complex than open-field terrain scattering, radiative transfer models or discrete scatter formulations (Durden *et al.*, 1989) of forest backscatter from a sloping terrain have to be used to modify the open-terrain algorithm. Schuler *et al.* (1996) undertook experiments with airborne polarimetric P-band SAR data (6.6 m in range by 12.1 m in azimuth with 4 looks) over forested terrain with slopes up to 30° in the Black Forest, Germany. They obtained low RMSE (2° to 3°) and high correlation values for the measured slopes and the derived elevation profiles when compared to an accurate DEM. Attempts to use shorter wavelength radar (C- or L-bands) yielded profiles with larger errors for forested terrain, mainly for C-band. The larger slope estimation indicates that canopy and/or branch scattering dominates over the terrain relief scattering.

The technique was later applied with L-band SAR data over non-forested areas (Grandi *et al.*, 1997). A simplified closed form approximation to the relationship between the co-polarized maximum shift and the measured co-variance matrix elements is first established. Co-variance matrices generated from experimental or modelling data can then be used as input parameters to derive the link with the terrain azimuthal slope. Azimuthal direction slopes can then be computed from the polarimetric SAR data without any prior knowledge of the terrain. By integrating the slope profiles in the azimuthal direction relative terrain elevation can be derived. To obtain absolute elevation, one elevation point must be known along each slope profile.

To obtain two-dimensional topographic elevation and slope maps, sets of elevation profiles spaced throughout the range direction have to be available. Two orthogonal-pass SAR data provide a solution for generating an elevation surface with only one elevation-point (Grandi *et al.*, 1997). Shape-from-shading technique, which generates slopes in the across-track direction, could also be another solution.

To apply this technique with satellite SAR data (mainly C- and X-bands) future studies should be directed towards an analysis based on volume scattering to take into account the more complicated situation of the SAR backscattering with forested or agricultural areas. With such scattering models, quantitative slope and elevation values could be derived from the relationship between radiation frequency, incidence angle and type of scattering. However, the main drawbacks of this emergent technique are the volume scattering models but also the limited availability of polarimetric data to evaluate the robustness of the technique with different topographic and land cover situations.

5.3 Altimetry

There are two kinds of altimeter: the laser and the radar. The laser scanner represents an advanced method for topographic mapping. It could replace aerial photography in a short-term period, since laser represents an emerging technology that is making its transition from the proof-of-concept, prototype stage to a readily available and reliable commercial survey instrument (Flood and Gutelius, 1997). Automatic DEM generation over large areas is thus produced in a short delivery time. Its use is mainly restricted to airborne platforms, although a proposal was done, without success, for a satellite laser altimeter of high resolution to map the polar ice sheets (Bufton *et al.*, 1982). The instrument would have also provided useful data on cloud-top heights and the ocean surface.

The satellite radar altimeter measures the height of a reflecting facet scanned by the passage of the instrument overhead. It uses the echo delays from within the pulse-limited footprint to estimate the minimum radar range (Moore and Williams, 1957). Outside of the pulse, a limited footprint for a flat surface is determined by the pulse length (Brown, 1962). As an example, the radar altimeter of GEOSAT has a pulse-limited footprint of about 2 km in diameter, which increases to many kilometres as large-scale surface roughness increases. Other system limitations (inaccuracies in the timing, tropospheric and ionospheric delays of the radar wave propagation and orbit determination errors) introduce errors in the range precision, which indirectly affects the spatial resolution. However, a dual-frequency altimeter should correct out the residual ionospheric uncertainty (Goldhirsh and Rowland, 1982). Since orbit errors are usually regarded as long wavelength phenomena (40,000 km) least square adjustment using trend and bias parameters are other methods to reduce errors at cross-points between ascending and descending orbit passes (Noréus, 1995).

The two main disadvantages of conventional radar altimeters are the large footprint and its dilation with rougher terrain. A third disadvantage is that most of the radiated power falls outside of the footprint and cannot be used for height estimations. Although the radar altimeter can measure distances within 10 cm, these drawbacks have presently reduced its applications to

flat surfaces such as the ocean surface and the ice sheets. The delay/Doppler radar altimeter (Raney, 1998) should overcome some of these difficulties:

(i) More equivalent looks are accumulated to achieve a relatively small along-track footprint size (on the order of 250 m for a Ku-band altimeter). This minimizes unwanted terrain dependency of the footprint size and position, and

(ii) The entire along-track signal history contributes to height measurements rather than only the small pulse-limited area. It used much more of the instrument's radiated energy, and then increases the efficiency of the system.

Measuring the distance between the satellite and the ground is only the first step of a longer procedure to convert it into an elevation relative to the geoid (Robinson, 1985). The geoid is the equipotential surface at mean sea level, with regards to Earth's gravitation only. The other gravitational attractions (such as those of the sun, the moon, etc.) are classified as perturbations, which give rise to the height of the sea surface relative to the geoid.

Furthermore, the geoid is in general approximated by an ellipsoid, which deviates in height from the geoid by distances of about 50 m due to uneven mass distribution, and the satellite orbit is determined relative to the reference ellipsoid. Therefore both measurements (height above the sea-surface and satellite orbit relative to ellipsoid) have to be obtained with the same degree of accuracy. In fact, errors in the final sea-surface height (above the geoid) calculation arises from inaccuracies in the modelling of the satellite orbit (Robinson, 1985). To reduce this error the satellite should have as many ground-tracking stations as possible with globally dispersed coverage. Now the use of GPS provides sufficiently accurate means for determining the position of the altimeter satellite relative to the ellipsoid.

To finally resolve ocean-surface topography the geoid shape relative to the reference ellipsoid should be known within 10-cm accuracy over the ocean length scales being studied. This is not possible at this time. In fact it is the reverse. Geodesists used satellite altimetry to map the geoid over the ocean with an accuracy of about 1 m. Consequently, the best geoid estimate by geodesists is not dependent on the sea-surface height that oceanographers want to extract (Brown *et al.*, 1983). For oceanographers, the time-varying aspects of ocean dynamics can thus be addressed with repeat orbits such as (i) the ocean currents or geostrophic balance (Pond and Pickard, 1983), (ii) ocean-circulation determination and tidal studies (Cartwright, 1983) and (iii) the ocean bathymetry (Marsh and Martin, 1982).

With GEOSAT, the large number of repeat orbits (up to 64) can be processed with a third-degree polynomial to adjust the residuals between repeated altimeter profiles and a mean height profile. This averaging procedure improves the determination of the mean topography of the sea surface with an effective precision determined to be 1.5 cm (Noréus, 1995). This can then be used to characterize gravity anomalies. Furthermore, short-wavelength orbit errors were also reduced. The method can also be applied on other data sources with many collinear tracks such as ERS-13-day and 35-day repeat cycle data and Topex/Poseidon. The use of multiple satellite data sets yields improved track coverage and increases the feasibility of recovering the height and consequently the geopotential field in the across-track direction.

Since the 1990's, the ERS-1 and Topex/Poseidon altimeters offer improved data quality and

global data coverage in comparison with the previous altimeters from GEOS-3, Seasat and GEOSAT. In combination with its other sensors, the ERS altimeter has been contributing to scientific development in the following areas of ocean dynamic research (ESA, 1995):

- improved description of 2-D surface waves and wave heights for wave forecasting;
- ocean topography from the mesoscale to the global scale; and
- ocean surface wind field measurement at high spatial resolution.

6.0 CONCLUDING REMARKS

Elevation modelling from satellite data has been a vibrant R&D topic for the last thirty years since the launch of the first civilian remote sensing satellite. Different data (space photographs, VIR scanner, SAR, altimeter) in different formats (analog, digital) can be processed by different methods (shadowing/shading; stereoscopy, interferometry, polarimetry) taking advantage of the different sensor and image characteristics (geometric, radiometric, phase) using different types of technology (analog, analytical, digital) and processing (interactive, automatic).

Most of the techniques have been proposed and tested in the early years. However, the limited availability of data and associated technologies has restricted their evolution in comparison with traditional photogrammetry. Their respective evolution is also a function of the research effort in terms of physical parameter modelling and data processing.

The shadowing method, providing localized cues along special contours is principally used to derive the relative elevation of a specific target. Despite good results the method remains limited to specific applications. Conversely to shadowing shading provides cues all over the studied surface, but can be applied successfully only on homogeneous surfaces. Combined with the empirical approach to resolve the different ambiguities, the method also remains marginal whatever the potential accuracy. Both methods have generated limited interest in the scientific community. On the other hand, stereoscopy is the most preferred and used method by the mapping, photogrammetry and remote sensing communities, most likely due to the heritage of the well-developed stereo photogrammetry. The latest advances in computer vision to model human vision have led to the advent of new automatic image processing approaches applied to satellite stereoscopy. Thus, the mapping process has become more automated, but not completely with occasional unmatched expectations. Inversely, radar altimetry and polarimetry have remained more at the level of scientific interest in the physical parametric modelling without much effort made in data or image processing development.

Whether certain methods evolve depends on the trends of scientific interest. SAR stereoscopy was popular around the 1980's with the development of radargrammetry equations and the first interesting and promising results with SIR-B. However, SAR image processing and related technologies to extract elevation data (such as image matching) were not mature enough and led to a temporary decline. In the same way, most of the R&D in shape-from-shading method was done in the 1980's starting with the Venus radar mapper. At the same time, there was an enormous interest in SPOT data with enormous research around the world both in physical parametric modelling and image processing, taking advantage also of the R&D in digital photogrammetry.

When ERS-1 was launched, scientists became enthusiastic over interferometric techniques using previously developed parametric modelling. Most research efforts have then focused in the first years on image processing (coherence image, phase unwrapping) and very few on the newly identified and poorly quantified physical artefacts (atmospheric conditions, sensor calibration). With the launch of RADARSAT in 1995, there is renewed interest in radargrammetry because researchers could take advantages of the R&D in image matching realized for SPOT at the end of the 1980's, and in the new computer technologies.

It seems obvious that the R&D of the new millennium will be focused on the use of the high-resolution satellites (VIR and SAR) and the development of their associated technologies. Already some research studies have looked at the stereoscopic potential of ASTER (Tokunaga *et al.*, 1996; Welch *et al.*, 1998) and of the US high-resolution satellites (Ridley *et al.*, 1997; Kaufmann *et al.*, 1997; Li, 1998), or the interferometric potential of SRTM (Werner, 1997). Already some data acquired from these types of new satellites (ASTER, KOMSAT, IKONOS, SRTM, etc.) are used to demonstrate their real potential for topographic mapping.

Since any sensor, system or method has its own advantages and disadvantages, solutions to be developed in the future for operational DEM generation should exploit the complementarity between the different sensors, methods and processing. It has already been optimized in stereoscopy combining VIR and SAR data where the radiometric content of the VIR image is combined with the SAR's high sensitivity to the terrain relief and its "all-weather" capability to obtain the second image of the stereo-pair.

With the same method, some complementary aspects can be applied:

- two SAR stereoscopic pairs from ascending and descending orbit paths to partially complement the backslopes of each stereo-pair;
- two interferometric pairs, one with a small baseline (to help the phase unwrapping), and the other with a larger baseline (to increase the accuracy); and
- two polarimetric images from ascending and descending orbit paths to resolve the across-track ambiguity and reduce the required number of known elevation points.

The complementarity of methods has already been tried with SAR where stereoscopy is used to generate seed points needed for the clinometry or to generate an approximate DEM to help the phase unwrapping in interferometry. The loss of coherence in interferometry in forested areas can be completed with clinometry, which is well suited to the homogeneity of the forest cover. Clinometry and polarimetry could be combined since the first one gives elevation information in the illumination direction and the second one in the azimuthal direction. Only one polarimetric SAR image would thus be necessary. The shadowing method to extract building or tree heights could also be used to reduce a stereoscopic or interferometric digital surface model (DSM) in a DEM, or inversely. DSMs of cities can be used in various applications related to geographic information systems.

The complementarity can also apply at the processing level: (i) using the visual matching to seed points to the automatic matching or to post-process and edit raw DEMs (occlusion, shadow or

mismatched areas); or (ii) using stereo measurements of geomorphological features (thalweg and crest lines, lakes surfaces, etc.) to increase the mapping consistency of the DEM. Furthermore, it has been proven in most of the previous experiments that the user has to make judgements and decisions at different stages of the processing, regardless of the level of automatic processing to obtain the final DEM product: the "know-how" of the users could favourably complement the computer capability in different processing steps.

In the past, high-quality DEMs have been generated with traditional photogrammetry in such a way that they were used for many purposes. Presently, DEMs are considered the most permanent and reusable geo-related data set over time. Although the need, requirements and specifications of DEM products are difficult to determine due to its multiple uses by different users' community, a global DEM generation is realized with the US/German Space Radar Laboratory embarking on a US shuttle mission, the SRTM launched in February 2000. It uses two-frequency single-pass interferometry with a second receiving antenna to generate DEMs over all land surfaces between -56º and +60º latitudes (Jordan *et al.*, 1995; Werner, 1997). The accuracy of the released DEM generated by the US C-band radar interferometry should be in the order of DTED level-1 accuracy. The accuracy of the DEM generated by German X-band radar interferometry will be slightly better, but with only a partial coverage of the landmass.

Is then a global DEM with a unique specification not a "wager"? Are these output statistics describing the global DEM helpful enough? Can we accept DEMs, which cannot produce "good-looking contour lines" in a mapping sense? Are we satisfied nowadays in producing "throwaway DEMs" at a particular scale that are maybe just good for a specific application? Will it fulfil the requirements of all DEM users? The other satellite data resellers hope not, since many new satellites with high-resolution VIR or SAR images with along- or across-track stereo capability are launched in the same time frame by US, Canadian, European, Indian, Russian, Japanese, etc., private or governmental organizations.

ABBREVIATIONS AND ACRONYMS

2D	Two Dimensional
3D	Three Dimensional
ACSM	American Congress on Surveying and Mapping
ADRO	Applications Development and Research Opportunity
ASPRS	American Society of Photogrammetry and Remote Sensing
ASTER	Advanced Spaceborne Thermal Emission and Reflection Radiometer
AVHRR	Advanced Very High Resolution Radiometer
B/H	Base-to-Height Ratio
CNES	Centre National d'Etudes Spatiales
CSA	Canadian Space Agency
DEM	Digital Elevation Model
DTED	Digital Terrain Elevation Data
DSM	Digital Surface Model
ERS	European Remote Sensing Satellite
ESA	European Space Agency
ETC	Earth Terrain Camera

FMC	Forward Motion Compensation
GCP	Ground Control Point
HRV	High Resolution in the Visible
ICP	Independent Check Point
IGN	Institut Géographique National
IRS	Indian Remote Sensing Satellite
JERS	Japan Earth Resources Satellite
LFC	Large Format Camera
LISS	Linear Imaging Self-scanned Sensor
MC	Metric Camera
MIT	Massachusetts Institute of Technology
MOMS	Modular Opto-Electronic Multispectral Scanner
MSS	Multi Spectral Scanner
NASA	National Aeronautics and Space Administration
NOAA	National Oceanic and Atmospheric Administration
OPS	Optical Sensor
PEPS	Preliminary Evaluation Program of SPOT
R&D	Research and Development
RMS	Root Mean Square
RMSE	Root Mean Square Error
SAR	Synthetic Aperture Radar
SIR	Spaceborne Imaging Radar
SPOT	Système pour l'Observation de la Terre
SRTM	Shuttle Radar Topography Mission
TM	Thematic Mapper
USA	United States of America
USGS	United States Geological Survey
USSR	Union of the Socialism Soviet Republics
VIR	Visible and Infra-Red

ACKNOWLEDGEMENTS

The author would like to thank his CCRS friends Drs. Brian Brisco, Bert Guindon, Laurence Gray, Karim Mattar and Ridha Touzi for the time they spent to review and improve this paper. Valuable comments on the manuscript were given by the anonymous external reviewer.

REFERENCES

Abbasi-Dezfouli, M. and T.G. Freeman, "Stereo-Images Registration Based on Uniform Patches", International Archives of Photogrammetry and Remote Sensing, Vienna, Austria, 31 (B2), 101-106 (1996).

Ackerman, F., D. Fritsch, M. Hahn, F. Schneider and V. Tsingas, "Automatic Generation of Digital Terrain Models with MOMS-02/D2 Data", Proceedings of the MOMS-02 Symposium, Köln, Germany, 5-7 July, 79-86 (1995).

Akeno, K., "DEM Generation from Multi-sensor Stereo-pairs AVHRR and MSS", International Archives of Photogrammetry and Remote Sensing, Vienna, Austria, 31 (B4), 36-40 (1996).

Al-Roussan, N. and G. Petrie, "System Calibration, Geometric Accuracy Testing and Validation of DEM and Ortho-Image Data Extracted from SPOT Stereo-Pairs Using Commercially Available Image Processing Systems", International Archives of Photogrammetry and Remote Sensing, Stuttgart, Germany, 32 (4), 8-15 (1998).

Al-Roussan, N., P. Cheng, G. Petrie, Th. Toutin and M.J. Valadan Zoej, "Automated DEM Extraction and Ortho-Image Generation from SPOT Level-1B Imagery", Photogrammetric Engineering and Remote Sensing, 63 (8), 965-974 (1997).

Audet, H. et A. Lapierre, «Revue des systèmes et techniques de visualisation stéréoscopique et de leur application en géomatique», Comptes-rendus du seizième Symposium canadien sur la télédétection, Sherbrooke, Québec, Canada, 7-10 juin, 449-454 (1993).

Baker, H.H. and T.O. Binford, "Depth from Edge and Intensity Based Stereo", Proceedings of the Seventh International Joint Conference on Artificial Intelligence, Vancouver, B.C., Canada, 631-636 (1981).

Bemis, S.V., J.L. Leeds and E.A. Winer, "Operator Performance as a Function of Type of Display: Conventional Versus Perspective", Human Factors, 30, 162-169 (1988).

Bloom, A.L., E.J. Fielding and X.-Y. Fu, "A Demonstration of Stereo-Photogrammetry with Combined SIR-B and Landsat-TM Images", International Journal of Remote Sensing, 9 (5), 1023-1038 (1988).

Boisvert, J.B., T. Pultz, R.J. Brown and B. Brisco, "Potential of Synthetic Aperture Radar for Large Scale Soil Moisture Monitoring: A Review", Canadian Journal for Remote Sensing, 22 (1), 2-13 (1995).

Brivio, P.A., A. Della Ventura, A. Rampini and R. Schettini, "Automatic Selection of Control Points from Shadow Structures", International Journal of Remote Sensing, 13 (10), 1853-1860 (1992).

Brown, G.S., "The Average Impulse Response of a Rough Surface and its Application", IEEE Transactions on Antennas Propagation, AP-25 (1), 67-74 (1962).

Brown, R.G., W.D. Kahn, D.C. McAdoo and W.E. Himwich, "Roughness of the Marine Geoid From Seasat Altimetry", Journal of Geophysical Research, 88C, 1531-1540 (1983).

Buchroithner, M., "Stereo-viewing from Space", Advances in Space Research, 19 (1), 29-40 (1989).

Bufton, J.L., J.E. Robinson, M.D., Femiano and F.S. Flatow, "Satellite Laser Altimeter for

Measurement of Ice Sheet Topography", IEEE Transactions on Geoscience and Remote Sensing, GE-20 (4), 544-549 (1982).

Canadian Space Agency, "Bringing Radar Application Down to Earth", Proceedings of the RADARSAT ADRO Symposium, Montreal, Canada, October 13-15, CD-ROM (1998).

Carlson, G.E., "An Improved Single Flight Technique for Radar Stereo", IEEE Transactions on Geoscience Electronics, GE-11, 199-204 (1973).

Cartwright, D.E., "Detection of Large-Scale Ocean Circulation and Tides", Phil. Transactions Royal Society London, A309, 361-370 (1983).

Centre National d'Études Spatiales (CNES), «SPOT-1 : Utilisation des images, bilan, résultats», Proceedings of the SPOT-1 Symposium, Paris, France, 1551 pages (1987).

Centre National d'Études Spatiales (CNES), «Le mouvement de véhicule spatial en orbite», Toulouse, France, 1031 pages (1980).

Cheng, F., and K.-H. Thiel, "Delimiting the Building Heights in a City from the Shadow in a Panchromatic Image-Part 1: Test of 42 Buildings", International Journal of Remote Sensing, 16 (3), 409-415 (1995).

Cheng, Ph., Th. Toutin and C. Stohr, "Automated DEM Extraction from Air Photos or Optical Satellite Images", Proceedings of the 13th International Conference "Applied Geologic Remote Sensing", Vancouver, BC, March 1-3, 1999 , Vol. 1 , pp. 56-63.

Cheng, Ph., and Th. Toutin, "Unlocking the Potential for IRS-1C Data", Earth Observation Magazine, 7 (3), 24-26 (1998).

Cooper, P., R., D.E. Friedman and S.A. Wood, "The Automatic Generation of Digital Terrain Models from Satellite Images by Stereo", Acta Astronautica, 15 (3), 171-180 (1987).

Day, T. and J.-P. A. Muller, "Quality Assessment of Digital Elevation Models Produced by Automatic Stereo-Matchers from SPOT Image Pairs", Photogrammetric Record, 12 (72), 797-808 (1988).

De Grandi, G. F., D.L. Schuler, T.L. Ainsworth and J.S. Lee, "Topography Sensing by Polarimetric SAR: Theoretical Basis and Application Using Orthogonal-Pass AIRSAR Data", Proceedings IGARSS'97, Singapore, August 11-15, 1371-1375 (1997).

Della Ventura, A., A. Rampini and R. Schettini, "Image Registration by Recognition of Corresponding Structures", IEEE Transactions on Geoscience and Remote Sensing, 28 (3), 305-314 (1990).

Denis, P., «Génération de modèle numérique de terrain à partir de données SPOT», International Archives of Photogrammetry and Remote Sensing, Lappia-House, Finland, August 19-

22, 26 (B3/2) 176-185 (1986).

Djamdji, J.-P. and A. Bijaoui, "Disparity Analysis: A Wavelet Transform Approach", IEEE Transactions on Geoscience and Remote Sensing, 33 (1), 67-76 (1995).

Domik, G., F. Leberl and J. Cimino, "Dependence of Image Grey Values on Topography in SIR-B Images", International Journal of Remote Sensing, 19 (5), 1013-1022 (1988).

Domik, G., "Evaluation of Radar Stereoviewability by Means of Simulation Techniques", Proceeding IGARSS'84, Paris, France, ESA-SP-215, 623-646 (1983).

Dorrer, E., W. Maier and V. Uffenkamp, "Stereo Compilation of MOMS-02 Scenes on the Analytical Plotter", Proceedings the MOMS-02 Symposium, Köln, Germany, 5-7 July, 95-110 (1995).

Dowman, I.J., Z.-G. Twu and P.H. Chen, "DEM Generation from Stereoscopic SAR Data", Proceedings of ISPRS Joint Workshop on Sensors and Mapping from Space, Hannover, Germany, September 29-October 2, 113-122 (1997).

Dowman, I.J., H. Ebner and C. Heipke, "Overview of European Developments in Digital Photogrammetric Workstations", Photogrammetric Engineering and Remote Sensing, 58 (1), 51-56 (1992).

Doyle, F., "A Large Format Camera for Shuttle", Photogrammetric Engineering and Remote Sensing, 45 (1), 73-78 (1979).

Ducher, G., "Metric Camera Data: Assessment and Potential Use at L'Institut Géographique National", Photogrammetric Record, 11 (66), 671-689 (1985).

Durden, S.L., J.J. van Zyl and H.A. Zebker, "Modelling and Observation of Radar Polarization Signature of forested Areas", IEEE Transactions on Geoscience and Remote Sensing, 27 (3), 290-301 (1989).

Ehlers, M. and R. Welch, "Stereo-Correlation of Landsat-TM Images", Photogrammetric Engineering and Remote Sensing, 53 (9), 1231-1237 (1987).

ESA – European Space Agency, "New Views of the Earth: Scientific Achievements of ERS-1", ESA SP1176/I Report, Paris, France, 162 pages (1995).

Escobal, P.R., "Methods of Orbit Determination", Krieger Publishing Company, Malabar, Florida, USA, 479 pages (1965).

Flood, M. and B. Gutelius, "Commercial Implications of Topographic Terrain Mapping using Scanning Airborne Laser Radar", Photogrammetric Engineering and Remote Sensing, 63 (4), 327-329 & 363-366 (1997).

Flusser, J. and T. Suk, "A Moment-Based Approach to Registration of Images with Affine Geometric Distortions", IEEE Transactions on Geoscience and Remote Sensing, 32 (2), 382-387 (1994).

Forster, R.R., K.C. Jezek, H. Gyoo Sohn, A.L. Gray and K.E. Mattar, "Analysis of Glacier Flow Dynamics from Preliminary RADARSAT InSAR Data of the Antarctic Mapping Mission", Proceedings of IGARSS'98, Seattle, USA, July 6-10, 2225-2227 (1998).

Förstner, W., "On the Geometric Precision of Digital Correlation", International Archives of Photogrammetry, Helsingfors, 24 (B3), 176-189 (1982).

Frankot, T.R., and R. Chellapa, "A Method for Enforcing Integrability in Shape from Shading", IEEE Transactions on Pattern Analysis and Machine Intelligence", 10 (4), 439-451 (1988).

Frankot, T.R., and R. Chellapa, "Estimation of Surface Topography from SAR Imagery Using Shape from Shading Techniques", Artificial Intelligence, 43, 271-310 (1990).

Friedhoff, R.M. and W. Benzon, "The Second Computer Revolution: Visualization", W.H. Freeman and Company, New York, USA, 214 pages (1991).

Fullerton, J.K., F. Leberl and R.E. Marque, "Opposite Side SAR Image Processing for Stereo-viewing", Photogrammetric Engineering and Remote Sensing, 52 (9), 1487-1498 (1986).

Gabriel, A.K., R. Goldstein and H. Zebker, "Mapping Small Elevation Changes Over Large Areas: Differential Radar Interferometry", Journal of Geophysical Research, 94 (B7), 9183-9191 (1989).

Gabriel, A.K. and R.M. Goldstein, "Crossed-Orbit Interferometry: Theory and Experimental Results from SIR-B", International Journal of Remote Sensing, 9 (5), 857-872 (1988).

Geudtner, D., P.W. Vachon, K.E. Mattar and A.L. Gray, "RADARSAT Repeat-Pass SAR Interferometry: Results over an Arctic Test Site", Proceedings of the GER'97 Symposium: Geomatics in the Era of RADARSAT, Ottawa, Canada, May 25-30, CD-ROM (1997).

Goldhirsh, J. and J.R. Rowland, "A Tutorial Assessment of Atmospheric Height Uncertainties for High-Precision Satellite Altimeter Missions to Monitor Ocean Currents", IEEE Transactions on Geoscience and Remote Sensing, GE-20 (4), 418-433 (1982).

Goldstein, R.M., H. Engelhardt, B. Kamb and R.M. Frolich, "Satellite Radar Interferometry for Monitoring Ice Sheet Motion: Application to an Antartic Ice Stream", Science, 262, 1525-1530 (1993).

Goldstein, R.M., H. Zebker and C. Werner, "Satellite Radar Interferometry: Two-Dimensional Phase Unwrapping", Radio Science, 23 (4), 713-720 (1988).

Gracie, G., J.W. Bricker, R.K. Brewer and R.A. Johnson, "Stereo Radar Analysis", Fort Belvoir, VA, USA, U.S. Engineering Topography Laboratory, Report FTR - 1339-1 (1970).

Graham, L.C., "Synthetic Interferometer Radar for Topographic Mapping", Proceedings of the IEEE, 62 (6), 763-768 (1974).

Gray, A.L., K.E. Mattar, P.W. Vachon, R. Bindschadler, K.C. Jezek and R. Forster, "InSAR Results from the RADARSAT Antarctic Mapping Mission Data: Estimation of Glacier Motion Using a Simple Registration procedure", Proceedings of IGARSS'98, Seattle, USA, July 6-10, III, 1638-1640 (1998).

Grün, A., "Digital Photogrammetric Stations: A Short List of Unmatched Expectations", Geo Info Magazine, 11 (1), 20-23 (1997).

Gugan, D.J. and I.J. Dowman, "Accuracy and Completeness of Topographic Mapping from SPOT Imagery", Photogrammetric Record, 12 (72), 787-796 (1988).

Gugan, D.J., "Practical Aspects of Topographic Mapping from SPOT Imagery", Photogrammetric Record, 12 (69), 349-355 (1987).

Gugan, D.J., and I.J. Dowman, "Design and Implementation of a Digital Photogrammetric System", International Archives of Photogrammetry and Remote Sensing, 26 (B2), 100-109 (1986).

Guichard, H., «Étude théorique de la précision dans l'exploitation cartographique d'un satellite à défilement : application à SPOT», Bulletin de la Société Française de Photogrammétrie et de Télédétection, 90, 15-26 (1983).

Guichard, H., G. Ruckebusch, E. Sueur, S. Wormser, «Stéréorestitution numérique SPOT : une approche originale de formation des images épipolaires et de mise en correspondancce», Proceedings of the SPOT-1 Image Utilization, Assessment, Results, Paris, France, France, November, 1371-1392 (1987).

Guindon, B., "Development of a Shape-From-Shading Technique for the Extraction of Topographic Models from Individual Spaceborne SAR Images", IEEE Transactions on Geoscience and Remote Sensing, 28 (4), 654-661 (1990).

Hagberg, J.O., L.M.H. Ulander and J. Askne, "Repeat-Pass Interferometry Over Forested Terrain", IEEE Transactions on Geoscience and Remote Sensing, 33 (2), 331-340 (1995).

Hähn, M. and W. Förstner, "The Applicability of Feature-Based and a Least Squares Matching Algorithm for DEM Acquisition", International Archives for Photogrammetry and Remote Sensing, 27 (B9), III137-III150 (1988).

Hartl, Ph. and F. Cheng, "Delimiting the Building Heights in a City from the Shadow on a

Panchromatic SPOT Image: Part 2: Test of a Complete City", International Journal of Remote Sensing, 16 (15), 2829-2842 (1995).

Heipke, C., State-of-the-Art Digital Photogrammetric Workstations for Topographic Applications", Photogrammetric Engineering and Remote Sensing, 61 (1), 49-56 (1995).

Helava, U.V., "On System Concepts for Digital Automation", International Archives of Photogrammetry and Remote Sensing, 27 (B2), 171-190 (1988a).

Helava, U.V., "Object Space Least Squares Correlation", Proceedings of the ACSM-ASPRS Annual Convention, St. Louis, Missouri, USA, 3, 46-55 (1988b).

Hoffman, R.R., "Remote Perceiving: A Step Towards a Unified Science of Remote Sensing", Geocarto International, 5 (2), 3-13 (1990).

Horn, B. and M. Brooks (Editors), "Shape from Shading", The MIT Press, Cambridge, Massachusetts, USA, 577 pages (1989).

Horn, B., "Obtaining Shape from Shading Information", The Psychology of Computer Vision (Chapter 4), McGraw-Hill Book Company, New York, NY, USA, 115-155 (1975).

Hottier, Ph., et M. Albattah, «Transformation d'un couple de scènes SPOT en un couple d'images épipolaires analogiquement ou analytiquement restituable sans déformation du relief», Bulletin de la Société Française de Photogrammétrie et de Télédétection 123, 13-27 (1991).

Huertas, A., and R. Nevatia, "Detecting Building in Aerial Images", Computer Vision, Graphics and Image Processing, 41,131-152 (1988).

Jacobsen, K., "Calibration of IRS-1C Pan Camera", ISPRS Workshop on Sensors and Mapping from Space, Hannover, Germany, September 29 to October 2, 163-170 (1997).

Jacobsen, K. and W. Müller, "Evaluation of Space Photographs", International Journal of Remote Sensing, 9 (10-11), 1715-1721 (1988).

Jordan, R.L., B.L. Huneycutt and M. Werner, "The SIR-C/X-SAR Synthetic Aperture Radar", IEEE-Transactions on Geoscience and Remote Sensing, 33 (4), 829-839 (1995).

Kaufmann, V., und W. Sulzer, "Über die Nutzungsmöglichkeit hochauflösender amerikanischer Spionage-Satellitenbilder (1960-1972)", Vermessung und Geoinformation, Heft 3/97, 166-173 (1997).

Kaupp, V., L. Bridges, M. Pisaruk, H. MacDonald and W. Waite, "Simulation of Spaceborne Stereo Radar Imagery: Experimental Results", IEEE Transactions on Geoscience and Remote Sensing, 21 (2), 400-405 (1983).

Keidel, W., "Application and Experimental Verification of an Empirical Backscattering Cross-Section Model for the Earth's Surface", IEEE Transactions on Geoscience and Remote Sensing, 20 (1), 67-71 (1982).

Khizhnichenko, V.I., "Co-ordinates Transformation When Geometrically Correcting Earth Space Scanner Images", (in Russian) Earth Exploration From Space 5, 96-103 (1982).

Kobrick, M., F. Leberl and J. Raggam, "Radar Stereo Mapping with Crossing Flight Lines", Canadian Journal of Remote Sensing, 12 (9), 132-148 (1986).

Konecny, G., P. Lohmann, H. Engel and E. Kruck, "Evaluation of SPOT Imagery on Analytical Photogrammetric Instruments", Photogrammetric Engineering and Remote Sensing, 53 (9), 1223-1230 (1987).

Konecny, G., E. Kruck, and P. Lohmann, "Ein universeller Ansatz für die geometrische Auswertung von CCD-Zeilenabtasteraufnahmen", Bildmessung und Luftbildwesen, 54 (4), 139-146 (1986).

Kornus, W., M. Lehner, H. Ebner, H. Froba, T. Ohlhof, "Photogrametric Point Determination and DEM Generation Using MOMS-2P/PRIRODA Three-Line Imagery", International Archives for Photogrammetry and Remote Sensing, Stuttgart, Germany, Sept. 7-10, 32 (B4), 321-328 (1998).

Kostka, R., "Anwendungsbezogene Untersuchungen an Weltraum Photos von Gebirgsregionen" Mitteillungen der Forstlichen Bundesversuchsanstalt, Wien, Heft 157, 139-146 (1986).

Kratky, W., "On-line Aspects of Stereophotogrammetric Processing of SPOT Images", Photogrammetric Engineering and Remote Sensing, 55 (3), 311-316 (1989).

Kratky, W., "Rigorous Stereo Photogrammetric Treatment of SPOT Images", Proceedings of the SPOT-1 Image Utilization, Assessment, Results, Paris, France, France, November, 1281-1288 (1987).

La Prade, G., S.J. Briggs, R.J. Farrell and E.S. Leonardo, "Stereoscopy", Chapter X of the Manual of Photogrammetry, Fourth Edition, ASP, Falls Church, USA, 519-544 (1980).

La Prade, G., "Subjective Considerations for Stereo Radar", Proceedings of the Thirty-sixth Annual Meeting of the American Society of Photogrammetry, Washington, D.C., USA, March 1-6, 640-651 (1970).

La Prade, G., and E. Leonardo, "Elevations from Radar Imagery", Photogrammetric Engineering, 35 (4), 366-371 (1969).

La Prade, G., "An Analytical and Experimental Study of Stereo for Radar", Photogrammetric Engineering, 29 (2), 294-300 (1963).

Leberl, F., K. Maurice, J.K. Thomas and M. Millot, “Automated Radar Image Matching Experiment”, ISPRS Journal of Photogrammetry and Remote Sensing, 49 (3), 19-33 (1994).

Leberl, F., “Radargrammetric Image Processing”, Artech House, Norwood, USA, 595 pages (1990).

Leberl, F., G. Domik, J. Raggam and M. Kobrick, “Radar Stereo-mapping Techniques and Applications to SIR-B Images of Mount Shasta”, IEEE Transactions on Geoscience and Remote Sensing, 24 (4), 473-481 (1986a).

Leberl, F., G. Domik, J. Raggam, J. Cimino and M. Kobrick, “Multiple Incidence Angle SIR-B Experiment Over Argentina: Stereo-Radargrammetric Analysis”, IEEE Transactions on Geoscience and Remote Sensing, 24 (4), 482-491 (1986b).

Leberl, F., “Accuracy Analysis of Stereo Side Looking Radar”, Photogrammetric Engineering and Remote Sensing, 45 (8), 1083-1096 (1979).

Leberl, F., “Imaging Radar Applications to Mapping and Charting”, Photogrammetria, 32 (3), 75-100 (1976).

Lemmens, M., “A Survey on Stereo-Image Matching Techniques”, International Archives for Photogrammetry and Remote Sensing, 27 (B8), V11-V23 (1988).

Li, R., 1998, “Potential of High-Resolution Satellite Imagery for National Mapping Products”, Photogrammetric Engineering and Remote Sensing, 64 (12), 1165-1170.

Li, F. and R.M. Goldstein, “Studies of Multi-Baseline Spaceborne Interferometric Synthetic Aperture Radars”, IEEE Transactions on Geoscience and Remote Sensing, 28 (1), 88-97 (1990).

Light, D.L., D. Brown, A. Colvocoresses, F. Doyle, M. Davies, A. Ellasal, J. Junkins, J. Manent, A. McKenney, R. Undrejka and G. Wood, “Satellite Photogrammetry”, in Chapter XVII of the Manual of Photogrammetry, American Society of Photogrammetry, 883-977 (1980).

Lodwick, G.H. and S.H. Paine, “A Digital Elevation Model of the Barnes Ice-Cap Derived from Landsat-MSS Data”, Photogrammetric Engineering and Remote Sensing, 51 (12), 1937-1944 (1985).

Lyon, R.J., “Remote Sensing: Visions Beyond Sight”, Stanford Today, Series 1 (17), 2-7 (1966).

Maître, H., F. Turpin et J.-M. Nicolas, «Cartographie automatique radar : l’apport du traitement d’images», Bulletin de la Société Française de Photogrammétrie et de Télédétection 148, 6-14 (1997).

Makarovic, B., "Analytical Versus Digital Photogrammetric Techniques and Systems", International Archives for Photogrammetry and Remote Sensing, 27 (B11), IV430-IV439 (1990).

Malleswara Rao, T., K. Venugopala Rao, A. Ravi Kumar, R.P. Rao and B.L. Deekshatula, "Digital Terrain Model from Indian Remote Sensing Satellite Data from The Overlap of Two Adjacent Paths Using Digital Photogrammetric Techniques", Photogrammetric Engineering and Remote Sensing, 62 (6), 726-731 (1996).

Manual of Photogrammetry, Fourth Edition, American Society of Photogrammetry, Falls Church, Va., USA (1980).

Manual of Remote Sensing, Third Editions, American Society of Photogrammetry and Remote Sensing, Falls Church, Va., USA (1998).

Marinelli, L., Th. Toutin et I. Downan, «Génération de MNT par radargrammétrie : état de l'art et perspectives», Bulletin de la Société Française de Photogrammétrie et de Télédétection, 148, 88-96 (1997).

Marr, D., "Vision: A Computational Investigation into the Human Representation and Processing of Visual Information", W.H. Freeman and Co., San Francisco, California, USA (1982).

Marr, D. and E. Hildreth, "A Theory of Edge Detection", Proceedings of the Royal Society of London, B207, 187-217 (1980).

Marr, D. and T. Poggio, "A Computation of Stereo Disparity", Proceedings of the Royal Society of London, B194, 283-287 (1977).

Marsh, J.G. and T.V. Martin, "The Seasat Altimeter Mean Surface Model", Journal of Geophysical Research, 87C, 3269-3280 (1982).

Maruyama, H., R. Kojiroi, T. Ohtsuka, Y. Shimoyama, S. Hara, and H. Masaharu, "Three Dimensional Measurement by JERS-1 OPS Stereo Data", International Archives for Photogrammetry and Remote Sensing, Athens, Ga, USA, 30 (B4), 210-215 (1994).

Masson, d'Autumne, G. de 1984, «Corrélation numérique d'images quelconques selon les lignes quasi-épilolaires par approximations successives», Bulletin de la Société Française de Photogrammétrie et de Télédétection, 95, 23-32 (1984).

Masson d'Autumne, G. de, «Le traitement géométrique des images de télédétection», Bulletin de la Société Française de Photogrammétrie et de Télédétection, 73-74, 5-16 (1979).

Massonnet, D., "Elevation Modelling and Displacement Mapping Using Radar Interferometry" in Chapter of Encyclopedia of Analytical Chemistry: Instrumentation and Applications",

John Wiley and Sons, Chichester, UK (2000).

Massonnet, D. and K. Feigl, "Discrimination of Geophysical Phenomena in Satellite Interferograms", Geophysical Research Letters, 22, 1537-1540 (1995).

Massonnet, D., M. Rossi, C. Carmona, F. Adragana, G. Peltzer, K. Feigl and T. Rabaute, "The Displacement Field of the Landers Earthquake Mapped by Radar Interferometry", Nature, 364, 138-142 (1993).

Massonnet, D. and T. Rabaute, "Radar Interferometry: Limits and Potential", IEEE Transactions on Geoscience and Remote Sensing, 31 (2), 455-464 (1993).

Meng, J., and M. Davenport, "Building Assessment with Sub-Pixel Accuracy Using Satellite Imagery", Proceedings SPIE, 2656, 65-76 (1996).

Meneguette, A.A.C., "Evaluation of Metric Camera Photography for Mapping and Co-ordinates Determination", Photogrammetric Record, 11(66), 699-709 (1985).

Moore, R.K., "Heights from Simultaneous Radar and Infrared", Photogrammetric Engineering, 5 (7), 649-651 (1969).

Moore, R.K. and C.S. Williams, "Radar Terrain Return at Near-Vertical Incidence", Proceedings of IRE, 45, 228-238 (1957).

Mott, R.K., "The Use of Satellite Imagery for Very Small Scale Mapping", Photogrammetric Record, 8 (46), 458-475 (1975).

Murai, S., "Cartographic accuracy of Stereo Space photographs Taken by Large Format Camera: a Case Study in Japan", Proceedings of ISPRS Symposium Mapping from Modern Imagery, Edinburgh, Scotland, September 8-12, 26 (B4), 732-737 (1986).

Noréus, J.P., "Improved Resolution of GEOSAT Altimetry Using Dense Sampling and Polynomial Adjusted Averaging", International Journal of Remote Sensing, 16 (15), 2843-2862 (1995).

Okoshi, T., "Three-Dimensional Imaging Techniques", Academic Press, New York, USA, 403 pages (1976).

Paderes, F.C., E.M. Mikhail and J.A. Fagerman, "Batch and On-line Evaluation of Stereo SPOT Imagery", Proceedings of the ASPRS-ACSM Convention, Baltimore, MD, USA, 3, 31-40 (1989).

Paillou, Ph. and M. Gelautz, "Relief Reconstruction from SAR Stereo Pairs : The Optimal Gradient Matching Method", IEEE Transactions on Geoscience and Remote Sensing, 37 (4), 2099-2107 (1999).

Paquerault, S., et H. Maître, «La radarclinométrie», Bulletin de la Societé Française de Photogrammétrie et de Télédétection, 148, 20-29 (1997).

Parashar, S., E. Langham, J. McNally and S. Ahmed, "RADARSAT Mission Requirements and Concepts", Canadian Journal of Remote Sensing, 19 (4), 280-288 (1993).

Petit-Frère, J., «Prise en compte des différences photométriques entre images dans les techniques de stéréorestitution», International Archives of Photogrammetry and Remote Sensing, Washington, D.C., USA, 29 (B4), 392-398 (1992).

Petrie, G., "Trends in Analytical Instrumentation", ITC Journal, 1992-4, 364-383 (1992).

Petrie, G., "Developments in Analytical Instrumentation", ISPRS Journal of Photogrammetry and Remote Sensing, 45, 61-89 (1990).

Polidori, L. et Th. Toutin, «Cartographie du relief par imagerie radar : l'état de l'art», Bulletin de la Societé Française de Photogrammétrie et de Télédétection, 152 (4), 12-23 (1998).

Polidori, L., «Cartographie radar», Gordon and Breach Science Publishers, Amsterdam, The Netherlands, 287 pages (1996).

Polidori, L., "Digital Terrain Models from Radar Images: a Review", Proceedings of the International Symposium on Radars and Lidars in Earth and Planetary Sciences, ESA SP-328, Cannes, France, September 2-4, 141-146 (1991).

Pond, S. and G.L. Pickard, "Introductory Dynamical Oceanography", Second Edition Pergamon Press, Oxford, United Kingdom (1983).

Priebbenow, R. and E. Clerici, "Cartographic Applications of SPOT Images", Proceedings of the SPOT-1 Image Utilization, Assessment, Results, Paris, France, November, 1189-1194 (1987).

Raggam, H., K. Gutjahr and A. Almer, "MOMS-2P und RADARSAT: Neue Sensoren zur stereometrischen Geländemodellerstellung", Vermessung und Geoinformation, Heft 4/97, 267-280 (1997).

Raggam J. and A. Almer, "Assessment of the Potential of JERS-1 for Relief Mapping Using Optical and SAR Data", International Archives of Photogrammetry and Remote Sensing, Vienna, Austria, 31 (B4), 671-676 (1996).

Raggam, J., A. Almer and D. Strobl, "A Combination of SAR and Optical Line Scanner Imager for Stereoscopic Extraction of 3-D Data", ISPRS Journal of Photogrammetry and Remote Sensing, 49 (4), 11-21 (1994).

Raggam, J., A. Almer, W. Hummelbrunner and D. Strobl, "Investigation of the Stereoscopic Potential of ERS-1 SAR Data", Proceedings of the Fourth International Workshop on

Image Rectification of Spaceborne Synthetic Aperture Radar", Loipesdorf, Austria, 26-28 May, 81-87 (1993).

Raggam, J. and A. Almer, "A Multi-Sensor Stereo-Mapping Experiment", Proceedings of the ACSM/ASPRS/Auto Carto Annual Convention Baltimore, MD, 4, 173-182 (1991).

Raggam, J. and F. Leberl, "SMART- a Program for Radar Stereo Mapping on the Kern DSR-1", Proceedings of the ASP-ACSM Annual Convention, Washington, D.C., March 11-16, 765-773 (1984).

Ramapriyan H., J. Strong, Y. Hung and C. Murray, "Automated Matching Pairs of SIR-B Images for Elevation Mapping", IEEE Transactions on Geoscience and Remote Sensing, 24 (4), 462-472 (1986).

Raney, R. K., "The Delay/Doppler Radar Altimeter", IEEE Transactions on Geoscience and Remote Sensing, 36 (5), 1578-1588 (1998).

Renouard, L., «Création automatique de MNT à partir de couples d'images SPOT», Proceedings of the SPOT-1 Image Utilization, Assessment, Results, Paris, France, France, November, 1347-1355 (1987).

Ridley, H.M., P.M. Atkinson, P. Aplin, J.-P. Muller and I. Dowman, "Evaluation of the Potential of the Forthcoming US High-resolution Satellite Sensor Imagery at the Ordnance Survey", Photogrammetric Engineering and Remote Sensing, 63 (8), 997-1005 (1997).

Rindfleisch, T., "Photometric Method for Lunar Topography", Photogrammetric Engineering, 32 (2), 262-277 (1966).

Robinson, I.S. "Satellite Oceanography: An Introduction for Oceanographers and Remote Sensing Scientists", Ellis Horwood Ltd., Chichester, UK, 455pages (1985).

Rodgers, A.E.E., and R.P. Ingalls, "Venus Mapping: The Surface Reflectivity by Radar Interferometry", Sciences, 165, 797-799 (1969).

Rosenfield, G.H., "Stereo Radar Techniques", Photogrammetric Engineering, 34, 586-594 (1968).

Rosenholm, D., "Numerical Accuracy of Automatic Parallax Measurement of Simulated SPOT Images", Canadian Journal of Remote Sensing, 12 (2), 103-113 (1986).

Saraf A.K., J.D. Das, B. Agarwal and R.M. Sundaram, "False Topography Perception Phenomena and its Correction", International Journal of Remote Sensing, 17 (18), 3725-3733 (1996).

Schuler, D.L., J.S. Lee and G. De Grandi, "Measurement of Topography Using Polarimetric SAR Images", IEEE Transactions on Geoscience and Remote Sensing, 34 (5), 1266-1277

(1996).

Shettigara, V.K. and G.M. Sumerling, "Height Determination of Extended Objects Using Shadows in SPOT Images", Photogrammetric Engineering and Remote Sensing, 64 (1), 35-44 (1998).

Simard, R. and Slaney, "Digital Terrain Model and Image Integration for Geologic Interpretation", Proceedings of the Fifth Thematic Conference on Remote Sensing for Exploration Geology, Reno, Nevada, USA, September 29-October 2, 49-60 (1986).

Simard R., Th. Toutin, A. Leclerc, S.R. Haja, M. Allam, R. Boudreau and R. Slaney, "Digital Terrain Modelling with SPOT Data and Geological Applications", Proceedings of the SPOT-1 Image Utilization, Assessment, Results, Paris, France, France, November, 1205-1212 (1987).

Simard R., F. Plourde and Th. Toutin, "Digital Elevation Modelling with Stereo SIR-B Image Data", Proceedings of the International Symposium on Remote Sensing for Resources Development and Environmental Management, ISPRS Commission VII, Enschede, The Netherlands, 161-166 (1986).

Simard, R., "Digital Stereo-Enhancement of Landsat-MSS Data", Proceedings of the Seventeenth International Symposium on Remote Sensing of Environment, Ann Arbor, MI, USA, May 9-13, 1275-1281 (1983).

Simard, R., «Résultats se simulations d'images stéréoscopiques HRV SPOT sur le sîte de Gun Lake, C. -B.», Proceedings of the Seventh Canadian Symposium on Remote Sensing, Winnipeg, Manitoba, Canada, September 8-11, 541-551 (1981).

Smith, J.A., T.L. Lin and K.H. Rawson, "The Lambertian Assumption and Landsat Data", Photogrammetric Engineering and Remote Sensing, 46 (9), 1183-1189 (1980).

Sylvander, S., D. Cousson et P. Gigord, «Étude des performances géométriques des images RADARSAT», Bulletin de la Société Française de Photogrammétrie et de Télédétection, 148, 57-65 (1997).

Teillet, P., B. Guindon and D. Goodenough, "On the Slope/Aspect Correction of Multispectral Scanner Data", Canadian Journal of Remote Sensing, 8 (2), 84-106 (1982).

Thomas, J., W. Kober and F. Leberl, "Multiple-Image SAR Shape from Shading", Proceedings IGARSS'89, Vancouver, Canada, July 10-14, 592-596 (1989).

Thomas, J. and W. Kober, "Radarclinometry – Shape from Shading: Generalized *N*-Image Algorithm", Sections 15.4 to 15.7 of "Radargrammetric Image Processing" by F. Leberl, Artech House, Norwood, USA, 435-551 (1990).

Tokunaga, M. and S. Hara, "Overview of DEM Product Generated by Using ASTER Data",

International Archive of Photogrammetry and remote Sensing, Vienna, Austria, 31 (B4), 874-878 (1996).

Toutin, Th. and S. Amaral, "Stereo RADARSAT Data for Canopy Height in Brazilian Forests", Canadian Journal for Remote Sensing, 25 (3), 189-199, (2000).

Toutin, Th., "Evaluation of Radargrammetric DEM from RADARSAT Images in High Relief Areas", IEEE Transactions on Geoscience and Remote Sensing, 38 (2), 782-789, (2000a).

Toutin, Th., "Stereo-Mapping with SPOT-P and ERS-1 SAR Images", International Journal of Remote Sensing, 21 (8), 1657-1674, (2000b).

Toutin, Th., "Error Tracking of Radargrammetric DEM from RADARSAT Images", IEEE Transactions on Geoscience and Remote Sensing, 37 (5), 2227-2238 (1999).

Toutin, Th. and C. Vester, "Radar and Stereoscopy Tutorial", Canada Centre for Remote Sensing Web site, http//www.ccrs.nrcan.gc.ca/ccrs/eduref/sradar/srintroe.html, (1998).

Toutin, Th., "Depth Perception with Remote Sensing Data", Proceedings of the Seventeenth EARSeL Symposium on Future Trends in Remote Sensing, Lingby, Denmark, 17-19 June 1997, 401-409 (1998a).

Toutin, Th., «Evaluation de la précision géométrique des images de RADARSAT», Canadian Journal of Remote Sensing, 24 (1), 80-88 (1998b).

Toutin, Th., "SPOT and Landsat Stereo Fusion for Data Extraction Over Mountainous Area", Photogrammetric Engineering and Remote Sensing, 64 (2), 109-113 (1998c).

Toutin, Th., D. Hoja, E. Höppner, A. Rémond and C. King, "GCPs Selection from Multi Source Data Over Mountainous Topography", Proceedings of IGARSS'98, Seattle, USA, July 6-10, 5, 2339-2341 (1998a).

Toutin, Th., Ph. Cheng, and K. Seidel, "Indian Remote Sensing Satellite: Geocoding and DEM Extraction", Proceedings of the 20th Canadian Symposium on Remote Sensing, Calgary, Alberta, Canada, May 10-13, 29-32 (1998b).

Toutin, Th., "Opposite-side ERS-1 SAR Stereo Mapping Over Rolling Topography", IEEE Transactions on Geoscience and Remote Sensing, 34 (2), 543-549 (1996).

Toutin, Th., "Generating DEM from Stereo Images with a Photogrammetric Approach: Example with VIR and SAR Data, EARSeL Journal Advances in Remote Sensing, 4 (2), 110-117 (1995).

Toutin, Th., and M. Beaudoin, "Real-Time Extraction of Planimetric and Altimetric Features from Digital Stereo SPOT Data using a Digital Video Plotter", Photogrammetric Engineering and Remote Sensing, 61 (1), 63-68 (1995).

Toutin, Th., Cl. Nolette, Y. Charbonneau et P.-A. Gagnon, «Stéreo-restitution interactive des données SPOT : description d'un nouveau système», Journal canadien de télédétection, 29 (2), 146-151 (1993).

Toutin, Th., «Analyse mathématique des possibilités cartographiques du système SPOT», Thèse de Docteur-Ingénieur, École Nationale des Sciences Géodésiques, St-Mandé, France, 163 pages (1985).

Toutin, Th., «Analyse mathématique des possibilités cartographique du satellite SPOT", Mémoire de DEA, École Nationale des Sciences Géodésiques, St-Mandé, France, 63 pages (1983).

Trinder, J.C., B.E. Donnelly and Kwok Leong Keong, "SPOT Mapping Software for Wild Aviolyt BC2 Analytical Plotter", Proceedings IGARSS'88, Edinburgh, UK, 12-16, September, 1801-1806 (1988).

Twu, Z.-G. and I. Dowman, "Automatic Height Extraction from ERS-1 SAR Imagery", International Archives of Photogrammetry and Remote Sensing, 31 (B2), 380-383 (1996).

Ulaby, F.T. and M.C. Dobson, "Handbook or Radar Backscattering Statistics for Terrain", Artech House, 357 pages (1988).

Vachon, P., D. Geudtner, L. Gray and R. Touzi, "ERS-1 Synthetic Aperture Radar Repeat-Pass Interferometry Studies: Implications for RADARSAT", Canadian Journal of Remote Sensing, 21 (4), 441-454 (1995).

Valadan Zoej, M.J. and G. Petrie "Mathematical Modelling and Accuracy Testing of SPOT Level-1B Stereo-Pairs", Photogrammetric Record, 16 (91), 67-82 (1998).

Valenzuela, G.R., "Scattering of Electromagnetic Waves From a Tilted Slightly-Rough Surface", Radio Science, 11 (3), 1057-1066 (1968).

Vigneron, C. et P. Denis, «Stéréorestitution d'images SPOT à l'aide du logiciel Traster IGN/Matra», Proceedings of the Eighteenth International Symposium on Remote Sensing of Environment, Paris, France, October 1-5, 455-464 (1984).

Vincent, K.V., M.A. True, P.K. Pleitner, "Automatic Extraction of High Resolution Elevation Data from SPOT Stereo Images", Proceedings of the SPOT-1 Image Utilization, Assessment, Results, Paris, France, France, November, 1339-1345 (1987).

Vincent, K.V., P.K. Pleitner, D.H. Coupland, H. Schultz and E.R.B. Oshel, "New Digital Elevation Mapping Software Applied to SPOT Simulation Data", Proceedings of the 1984 SPOT Symposium, Scottsdale, Az., USA, May 20-23, 92-97 (1984).

Walker, A.S. and G. Petrie, "Digital Photogrammetric Workstation", International Archives of Photogrammetry and Remote Sensing, Vienna, Austria, July 9-18, 31 (B2), 384-395 (1996).

Wegmüller, U. and Ch. Werner, "SAR Interferometric Signature of Forest", IEEE Transactions on Geoscience and Remote Sensing, 33 (2), 1153 - 1161 (1995).

Welch, R., T. Jordan, H. Lang and H. Murakani, "ASTER as a Source for Topographic Data in the Late 1990's", IEEE Transactions on Geoscience and Remote Sensing, 36 (4), 1282-1289 (1998).

Welch, R., R.T. Jordan and J.C. Luvall, "Geocoding and Stereo Display of Tropical Forest Multi-Sensor Datasets", Photogrammetric Engineering and Remote Sensing, 56 (10), 1389-1392 (1990).

Welch, R., " Desktop Mapping with Personal Computers", Photogrammetric Engineering and Remote Sensing, 55 (11), 1651-1662 (1989).

Welch, R., and C.P. Lo, "Heights Measurements from Satellite Images", Photogrammetric Engineering and Remote Sensing, 43 (10), 1233-1241 (1977).

Werner, M., "Shuttle Radar Topography Mission", Proceedings of ISPRS Workshop: Sensors and Mapping from Space, Hannover, Germany, Sept. 29-Oct. 2, 9-11 (1997).

Westin, T., "Photogrammetric Potential of JERS-1 OPS", International Archives of Photogrammetry and Remote Sensing, Vienna, Austria, 31(B4), 937-942 (1996).

Westin T., "Precision Rectification of SPOT Imagery", Photogrammetric Engineering and Remote Sensing, 56 (2), 247-253 (1990).

Whittington, I.F.G., "An Assessment of the Capability of Stereo Shuttle Photographs as a Source of Feature Content for Mapping", International Journal of Remote Sensing, 10 (6), 965-987 (1989).

Wildey, R.L., "Topography from Single Radar Images", Sciences, 224, 153-156 (1984).

Wildey, R.L., "Radarclinometry for the Venus Radar Mapper", Photogrammetric Engineering and Remote Sensing, 52 (1), 41-50 (1986).

Williams, J., "Geographic Information from Space", John Wiley and Sons, Chichester, U.K., 210 pages (1995).

Yelizavetin, I.V. and Ye. A. Ksenofontov, "Precision Terrain Measurement by SAR Interferometry", Mapping Sciences sand Remote Sensing, 33 (1), 1-19 (1996).

Yelizavetin, I.V., "Digital Terrain Modeling from Radar Image Stereopairs", Mapping Sciences

and Remote Sensing, 30 (2), 151-160 (1993).

Yoritomo, K., "Methods and Instruments for the Restitution of Radar Pictures", Invited Paper at the Twelfth Congress of the International Society for Photogrammetry, Ottawa, Canada, July 24-August 4 (1972).

Zebker, H.A., C. Werner, P.A. Rosen and S. Hensley, "Accuracy of Topographic Maps Derived from ERS-1 Interferometric Radar", IEEE Transactions on Geoscience and Remote Sensing, 32 (4), 823-836 (1994).